High Altitude Long Endurance UAV Analysis Model Development and Application Study Comparing Solar Powered Airplane and Airship Station-Keeping Capabilities

Thomas A. Ozoroski
Analytical Mechanics Associates, Hampton, Virginia

Craig L. Nickol and Mark D. Guynn
Langley Research Center, Hampton, Virginia

NASA STI Program . . . in Profile

Since its founding, NASA has been dedicated to the advancement of aeronautics and space science. The NASA scientific and technical information (STI) program plays a key part in helping NASA maintain this important role.

The NASA STI program operates under the auspices of the Agency Chief Information Officer. It collects, organizes, provides for archiving, and disseminates NASA's STI. The NASA STI program provides access to the NTRS Registered and its public interface, the NASA Technical Reports Server, thus providing one of the largest collections of aeronautical and space science STI in the world. Results are published in both non-NASA channels and by NASA in the NASA STI Report Series, which includes the following report types:

- TECHNICAL PUBLICATION. Reports of completed research or a major significant phase of research that present the results of NASA Programs and include extensive data or theoretical analysis. Includes compilations of significant scientific and technical data and information deemed to be of continuing reference value. NASA counter-part of peer-reviewed formal professional papers but has less stringent limitations on manuscript length and extent of graphic presentations.

- TECHNICAL MEMORANDUM. Scientific and technical findings that are preliminary or of specialized interest, e.g., quick release reports, working papers, and bibliographies that contain minimal annotation. Does not contain extensive analysis.

- CONTRACTOR REPORT. Scientific and technical findings by NASA-sponsored contractors and grantees.

- CONFERENCE PUBLICATION. Collected papers from scientific and technical conferences, symposia, seminars, or other meetings sponsored or co-sponsored by NASA.

- SPECIAL PUBLICATION. Scientific, technical, or historical information from NASA programs, projects, and missions, often concerned with subjects having substantial public interest.

- TECHNICAL TRANSLATION. English-language translations of foreign scientific and technical material pertinent to NASA's mission.

Specialized services also include organizing and publishing research results, distributing specialized research announcements and feeds, providing information desk and personal search support, and enabling data exchange services.

For more information about the NASA STI program, see the following:

- Access the NASA STI program home page at http://www.sti.nasa.gov

- E-mail your question to help@sti.nasa.gov

- Phone the NASA STI Information Desk at 757-864-9658

- Write to:
  NASA STI Information Desk
  Mail Stop 148
  NASA Langley Research Center
  Hampton, VA 23681-2199

High Altitude Long Endurance UAV Analysis Model Development and Application Study Comparing Solar Powered Airplane and Airship Station-Keeping Capabilities

Thomas A. Ozoroski
Analytical Mechanics Associates, Hampton, Virginia

Craig L. Nickol and Mark D. Guynn
Langley Research Center, Hampton, Virginia

January 2015

Acknowledgments

Contents

List of Tables

List of Figures

Abstract

There have been ongoing efforts in the Aeronautics Systems Analysis Branch at NASA Langley Research Center to develop a suite of integrated physics-based computational utilities suitable for modeling and analyzing extended-duration missions carried out using solar powered aircraft. From these efforts, SolFlyte has emerged as a state-of-the-art vehicle analysis and mission simulation tool capable of modeling both heavier-than-air (HTA) and lighter-than-air (LTA) vehicle concepts. This study compares solar powered airplane and airship station-keeping capability during a variety of high altitude missions, using SolFlyte as the primary analysis component. Three Unmanned Aerial Vehicle (UAV) concepts were designed for this study: an airplane (Operating Empty Weight (OEW) = 3285 kg, span = 127 m, array area = 450 m^2), a small airship (OEW = 3790 kg, length = 115 m, array area = 570 m^2), and a large airship (OEW = 6250 kg, length = 135 m, array area = 1080 m^2). All the vehicles were sized for payload weight and power requirements of 454 kg and 5 kW, respectively. Seven mission sites distributed throughout the United States were selected to provide a basis for assessing the vehicle energy budgets and site-persistent operational availability. Seasonal, 30-day duration missions were simulated at each of the sites during March, June, September, and December; one-year duration missions were simulated at three of the sites. Atmospheric conditions during the simulated missions were correlated to National Climatic Data Center (NCDC) historical data measurements at each mission site, at four flight levels. Unique features of the SolFlyte model are described, including methods for calculating recoverable and energy-optimal flight trajectories and the effects of shadows on solar energy collection. Results of this study indicate that: 1) the airplane concept attained longer periods of on-site capability than either airship concept, and 2) the airship concepts can attain higher levels of energy collection and storage than the airplane concept; however, attaining these energy benefits requires adverse design trades of reduced performance (small airship) or excessive solar array area (large airship).

1.0 Introduction

The lineage of this study traces to the early 2000's as the latest of several related research efforts undertaken by the Aeronautics Systems Analysis Branch (ASAB) at NASA Langley Research Center. In 2006, for example, a significant research effort investigated a wide range of potential Solar-Electric (SE) Unmanned Aerial Vehicle (UAV) types and technology candidates for High Altitude Long Endurance (HALE) missions. The results of the study were published in 2007 in a detailed 111-page report entitled, "High Altitude Long Endurance UAV Analysis of Alternatives and Technology Requirements Development" (NASA/TP-2007-214861, ref. 1). Other examples include the feasibility study for the UAV sector under the NASA Vehicle Systems Program, the ICESat mission quick-look study for the NASA Langley Systems Engineering Directorate, the hurricane hunter mission study for Langley's Science Directorate and, most recently, the Vulture mission analysis for DARPA.

As a by-product of supporting these past studies, research-level SE-HALE UAV analysis procedures had been developed within the ASAB; but inherent limitations indicated a strong need for new analysis capabilities. For example, the Airship Design and Analysis Code (ADAC, ref. 2) provided a narrowly focused capability for analyzing airship concepts; but ADAC could not be generalized or modified for use in most applications of interest. Other modeling deficiencies emerged when balancing conflicting fidelity levels or when implementing proprietary, restrictive, or stand-alone utilities within the analysis pathway. Overcoming these obstacles required adapting existing tools and procedures (sometimes with significant effort) to facilitate smooth interactions between those components suitable for the task at hand.

Shaped by the lessons learned from previous efforts, a computational analysis model was envisioned for meeting the unique vehicle analysis and mission simulation requirements of SE-HALE UAV concepts. Key applications of the model were projected to include the ability to analyze existing configurations, assess design sensitivities, conduct technology trades, and to simulate missions within time-variant solar and atmospheric operational environments. The model framework would provide coupled and recursive interactions between the analysis components to create the complexity needed to complete such studies. Furthermore, the model development would follow a spiraling pathway such that discrete, functioning versions would be completed, and then built upon, to create new versions with ever-increasing capability.

Thorough consideration of these requirements culminated in a concept summary document which prioritized modeling objectives, outlined the analysis framework, and mapped a general path toward completion. Within this context, a new analysis model was created and named *SolFlyte*, derived from the brief description, "**Sol**ar-electric **Fl**ight, including the effects of Energ**y** balance, **T**ime, and the **E**nvironment". Two separate analysis models were eventually completed, "SolFlyte-HTA" and "SolFlyte-LTA," for the analysis of heavier-than-air (HTA) and lighter-than-air (LTA) concepts, respectively. More details about the applicability, theory, and unique features of the SolFlyte analysis models are described in Section 3, including methods for calculating recoverable and energy-optimal flight trajectories and the effects of vehicle shadows on solar array energy collection.

This study compares solar powered airplane and airship station-keeping capability during a variety of high altitude missions, using SolFlyte as the primary analysis and simulation component. Three UAV concepts were designed for this study: an airplane (OEW = 3285 kg, span = 127 m, array area = 450 m^2), a small airship (OEW = 3790 kg, length = 115 m, array area = 570 m^2), and a large airship (OEW = 6250 kg, length = 135 m, array area = 1080 m^2). All the vehicles were sized for payload weight and power requirements of 454 kg and 5 kW, respectively. Seven mission sites distributed throughout the United States were selected to provide a basis for assessing the vehicle energy budgets and site-persistent operational availability. Seasonal, 30-day duration missions were simulated at each of the sites during March, June, September, and December; one-year duration missions were simulated at three of the sites. Atmospheric conditions during the simulated missions were correlated to National Climatic Data Center (NCDC) historical data measurements at each mission site, at four flight levels. The atmospheric data were corrected for measurement gaps based on adjustments to average measurements obtained during the specific simulation month and year at the mission site. Details of the HTA and LTA vehicle specifications, mission definitions, and assumptions utilized in this investigation are described in Section 4. An overview of the parametric design capabilities enabled by the SolFlyte solar energy collection analysis capabilities is also provided in that section.

2.0 Symbols

Sw – Wing Area

Vw – Wind Speed

Abbreviations

ADAC – Airship Design and Analysis Code

Alt% – Mission Altitude Metric

ASAB – Aeronautics Systems Analysis Branch

AvEnrg% – Mission Energy Availability Metric

deg – Degrees

E – East

ESS – Energy Storage System

HALE – High Altitude Long Endurance

H or HTA – Heavier-Than-Air

L or LTA – Lighter-Than-Air

Lat – Latitude

Lon – Longitude

N – North

NCDC – National Climatic Data Center

OEW – Operating Empty Weight

PwrRad% – Mission Power Capability Metric

S – South

SE – Solar Electric

TOGW –Takeoff Gross Weight

UAV – Unmanned Aerial Vehicle

WindData% – Mission Wind Data Suitability Metric

W – West

3.0 SolFlyte Modeling Scope and Theory

Developing a Complex Model

A meaningful first step towards a qualitative interpretation of the SolFlyte modeling approach is to describe differences between what might be termed *causal* and *complex* analysis models. Both models typically contain numerous interconnected components, of related mathematical and physical elements, that influence other components of the particular model. A *causal* model is also procedural, comprised of determinate components and determinate connectivity, with influences propagated sequentially and predictably from one component to the next. The analysis progresses in order from the first component to the last component unless feedback pathways were implemented in accordance with precisely known conditional operators. Results obtained from causal analysis models often can be improved by improving the fidelity of individual components and by enhancing the amount of information transferred between

components. In contrast, a *complex* model is ambiguous, comprised of various determinate, inexact, or unknown components. The connectivity is strongly coupled and influences are propagated throughout the model either sequentially or through similarly ambiguous feedback mechanisms, producing a reordered analysis sequence with indistinct start and end points. Existing connectivity and influence ambiguities block attempts to improve analysis model results by improving the fidelity of individual components.

Within this context, a causal model might be considered as the eventual limit of a complex model in which all components and connections have been clarified, but that transition is not always possible. For example, at the outset of SolFlyte development, it was evident that the vehicle geometry and performance combined with variable solar energy levels and uncertain weather conditions to generate complexity both within and between model components. As research and development progressed, other ambiguities appeared when considering:

- If, or how should, flight patterns be determined, connected, and influenced?
- What rules should be permitted to influence operations and therefore, results?
- Which analysis components are most important, and which can be omitted?

While attentive to complex modeling challenges, SolFlyte development necessarily expanded to address related concerns, such as clarifying vehicle and mission requirements definitions, identifying meaningful results metrics, and creating techniques for visualizing new types of results. The finalized SolFlyte concepts, capabilities, and assessement strategies now provide comprehensive guidance for future SE-HALE UAV vehicle and mission concept studies. A schematic diagram of the primary components and interactions of the SolFlyte analysis models is shown in Figure 1.
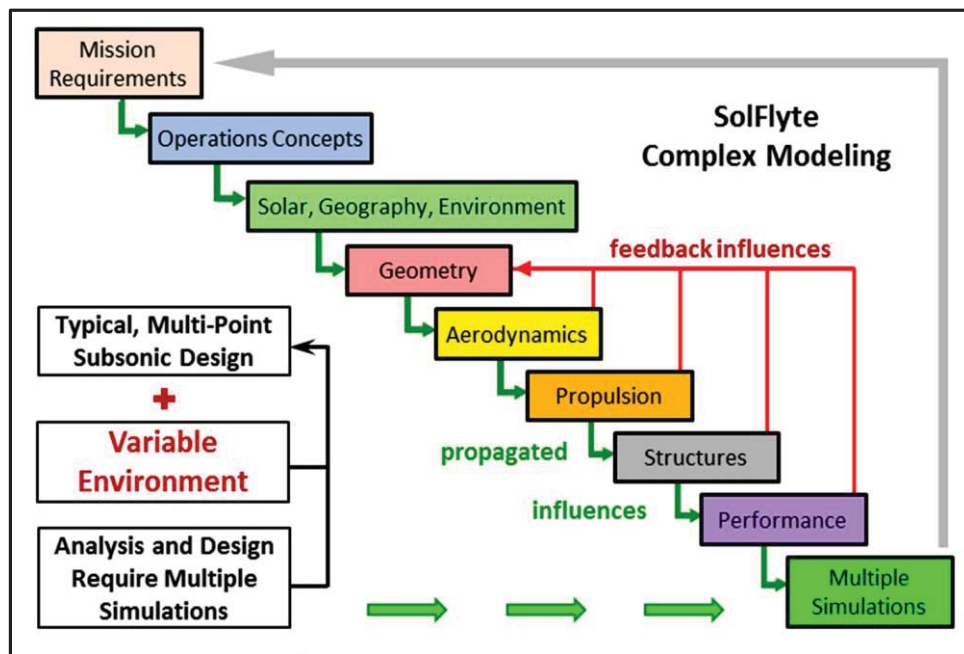
Figure 1. SE-HALE UAV model components and interactions.

SolFlyte Implementation and Practical Solutions

The SolFlyte tool is an integrated suite of functional utilities intended for concept-level analyses of solar-electric air vehicle and mission concepts, utilizing PHX ModelCenter® v9.0 as the integration framework. Within this particular framework, separate files, executable codes, and scripts are "wrapped" for use as analysis "components" and then linked to create an overall analysis "process model". There are two

separately applicable, but similar, process models for evaluating either airplane (SolFlyte-HTA) or airship (SolFlyte-LTA) concepts. These models also provide the functionality to simulate missions and assess the mission performance of the respective HTA and LTA concepts. Computational and procedural schemes were implemented to ensure that both analysis models would execute rapidly while retaining the ability to integrate the continually varying vehicle performance, energy levels, solar flux, and atmospheric conditions during each simulated mission time step. Addressing these considerations was enabled, in part, by creating three external modules: the "Wind Data Processing Model," the "Shadowing Assessment Utility," and the "Lighter-Than-Air Sizing Utility."

The Wind Data Processing Model is a separate process model designed for execution once at the outset of a study to automatically generate all formatted wind data files needed for subsequent mission analyses. The stand-alone Shadowing Assessment Utility is executed only once per vehicle geometry in order to generate a table of shadowing effects, caused by vehicle shadows cast upon the solar arrays, at roughly 36,000 Sun-vehicle orientations. The Shadowing Assessment Utility also provides a secondary capability to quickly calculate the shadowing effects at a single user-specified Sun-vehicle orientation. Finally, the Lighter-Than-Air Sizing Utility dually functions as a stand-alone airship design tool used prior to mission analyses, and then as an integrated, wrapped analysis component of the SolFlyte-LTA process model. The first application provides the capability to determine the vehicle size and system specifications, whereas the second application ensures that the specifications are correctly associated with the results of a particular mission simulation.

The analysis model execution time for the "Spokane, March, 30-Day, HTA-450" simulation presented in this report was 5 minutes, 11 seconds (64-bit operating system, with a 2.50 GHz processor, and 16.0 GB RAM). For this case, vehicle power requirements, shadowing, solar energy collection, and atmospheric conditions were determined at four flight levels, for 36 outbound headings, for a range of speeds incremented from stall to maximum, during each 15-minute simulated time step. The Wind Data Processing model can parse and format atmospheric data measurements from approximately 100 NCDC sites in about 30 minutes; the Shadowing Assessment Utility can generate a fully populated shadow table overnight, in about 9 hours; and the Lighter-Than-Air Sizing Utility can parametrically size an airship in about 1 second. The SolFlyte analysis models are configured to instantly access and extract information from the formatted wind data files and shadow tables during each simulation time step.

3.1 Features and Utilities

Principal features and concepts comprising the SolFlyte mission simulation and vehicle performance models are summarized in Sections 3.1.1 to 3.1.9. The descriptions of these features are intended to provide an overview of the flexibility, depth, and applicability of the SolFlyte models. Note that the functionality of the analysis capabilities described in these sections do not directly relate to individual components of the PHX ModelCenter® v9.0 process model framework.

3.1.1 Mission Site and Time Inputs

SolFlyte provides flexible input options to define and modify mission concepts. The mission start date, time of day, time step increment, and one or multiple mission sites should be selected to initiate each SolFlyte simulation. Site geography details stored in a wrapped Excel component are automatically accessed and updated by SolFlyte as the mission site counter is updated. Similarly, mission time progresses incrementally as the mission day and time-step counters are updated. A wide range of parameters are time dependent; to provide consistency during every time step of the simulated mission, all relevant astronomical, atmospheric, geographic, and vehicle status parameters are automatically updated or recalculated, as necessary. In addition, the numerical values of certain performance metrics are saved at

every time step for summation over the course of each simulated day and mission. Output is automatically saved as a separately named Excel file for each mission site.

3.1.2 Winds and Atmosphere Model

Prior to use in the SolFlyte analysis model, mission site details and mission atmospheric data during the mission time must be provided and saved as an Excel file. A separate "wind data" file is required for each mission site and the rows of data in the file must be specifically formatted and listed sequentially in time, by descending atmospheric pressure. Historical data files of validated atmospheric measurements can be downloaded from the National Climatic Data Center (NCDC) website and automatically processed by the Wind Data Processing utilities for assimilation with SolFlyte. More information about the NCDC wind data measurements and a list of approximately 1500 global sites can be found at the web address:

http://www1.ncdc.noaa.gov/pub/data/igra/ (accessed December, 2014)

The required and properly formatted atmospheric data input can originate from other sources, such as statistical models, or the user can choose to specify desired conditions. As described on the NCDC website, each row of processed mission wind data is ordered by columns as: wind year, month, day, hour, wind speed (m/s), wind direction (degrees clockwise, N = 0º), altitude (m), pressure (mb x 100), temperature (Kelvin), and density (kg/m^3 x 10^4). Note the mission start year and the wind data year are required mission simulation inputs, but they are independent parameters so numerical equality is not mandatory. Whether the data are supplied by the user or supplied automatically, atmospheric conditions associated with pressure altitudes of 100 mb, 70 mb, 50 mb, and 30 mb must be input for each year, month, and day. For a given day, the atmospheric data are listed sequentially, according to the data acquisition hour.

The Wind Data Processing model also extracts subsets of formatted NCDC site wind data to improve the analysis model execution time by narrowing data searches to a limited number of years. To further reduce analysis model execution time, SolFlyte creates smaller temporary files from the formatted subsets, viable only at the given mission site during the simulated mission time period. As a result, high-fidelity simulated atmospheric data is rapidly accessible for use in the SolFlyte analysis model during each mission time step at up to four different flight levels. The Wind Data Processing model is an external component of the SolFlyte model, requiring less than one hour to format about 100 NCDC data sites; a single execution creates the formatted wind data files required for all subsequent mission analyses.

Scrutiny of the NCDC historical atmospheric data can reveal data acquisition gaps or the existence of randomly occurring spurious measurement values. As a result, suitable historical data are not always available for all days and time steps of a desired mission time period. For this study, mission sites and wind data years were selected judiciously to minimize the possibility that data gaps could influence the results. For a few sites, however, a limited number of data gaps were identified during the desired mission wind data year and month. The data deficiencies were satisfactorily eliminated utilizing approximated median atmospheric values derived from measurements acquired at the site during other days of the mission year and month. For example, if the mission site atmospheric data were suitable for all but one day of a 30-day mission, the data gap was eliminated using approximated median conditions derived from measurements acquired during the other 29 days.

When historical wind data inputs are selected to initiate a mission simulation, the SolFlyte analysis model automatically identifies data deficiencies and inserts approximated median conditions unique to the mission site, month, and operational altitude. The analyst can select to refine or further substantiate the nominal tabulated values of approximated median conditions by analyzing measurements obtained during that same month, in different years.

6

3.1.3 On-Site Operational Radius Limits and Positioning Strategies

Station-keeping is a mission operational requirement that constrains the vehicle to execute persistent and recoverable flight patterns within a prescribed radial distance from a mission site. If the vehicle position at a given mission time is determined as within that radial distance, it is deemed as operating on-site; otherwise, it is deemed as operating off-site. The power-radius performance capability metric, *PwrRad%*, is the fraction of total mission time that the vehicle concept was determined as operating on-site, and it is calculated by summing values of the on-site status parameter during each time step of the simulated mission. The PwrRad% metric depends mostly on the vehicle maximum speed and the capability to withstand occasional strong winds; thus, it reflects the recoverable aspect of station-keeping.

To assess whether the vehicle is, in fact, operating on-site at a given mission time, concentric radial limits were defined as shown in Figure 2. In order of increasing distance from the origin, the operating regions bounded by these limits are shaded light green, dark green, and gray within an external red boundary. The mission site is depicted as a black disc at the origin of these circles. The inner-most light green region indicates satisfactory on-site positioning, whether or not the vehicle is operating upwind or downwind relative to the mission site. The darker green region extends beyond the inner region to indicate on-site positional energy reserves when operating upwind, and on-site positional energy deficits when operating downwind. The gray region indicates a vehicle radial position status that is temporarily unsatisfactory, but which could improve if the strong winds subside and if the vehicle can recover to an on-site region. The red boundary is the mission "cut-off" radius and identifies that the vehicle has been blown sufficiently far off-site that the mission would be aborted. During any time step, credit is awarded to the on-site status parameter only if the vehicle operating position is within either green region.
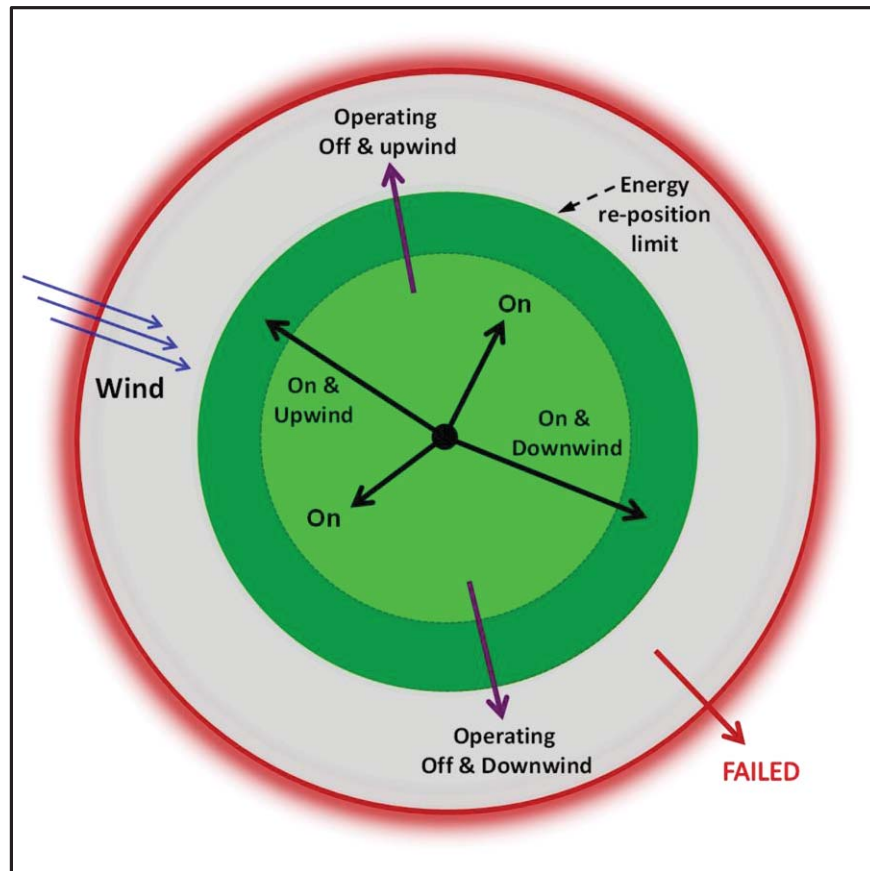

Figure 2. On-Site radius limits and definitions.

Although forecasted atmospheric conditions are assumed to be unknown for all missions of this study, it would be expected that forecast information could be utilized at any point during the mission to revise standard operational rules. One such example would be positioning the HTA vehicle upwind and on-site during light wind conditions to store potential (i.e., positional) energy, prior to the onset of strong winds. The strategy would also provide a means to adjust the timing, direction, and duration of impending off-site operations. Upwind energy positions are categorized as (+) and downwind energy positions are categorized as (–); both are inspected by the SolFlyte analysis model to determine appropriate standard operational strategies during the next time step.

Wind speeds are separated into categories that are defined differently for HTA and LTA vehicle concepts. For HTA concepts, light winds are defined as less than the vehicle stall speed, moderate winds are defined as greater than stall speed but less than maximum vehicle speed, and strong winds are defined as greater than the maximum vehicle speed. For LTA concepts, there are four wind speed category limits; the slowest speed limit is zero, followed by light and then moderate speed limits which are applied to input values greater than zero and less than the maximum vehicle speed, and the final speed limit is the maximum vehicle speed. Light and moderate LTA wind speeds are delineated by a user-supplied input variable that is typically set to a value less than about 5 m/s.

The *AvEnrg%* energy availability metric is the fraction of mission time that the vehicle concept maintains access to some combination of direct or stored energy *availability*. Thus, AvEnrg% reflects the *persistent* aspect of station-keeping, and is calculated by summing values of the energy status parameter during each time step of the simulated mission. Experience gained from various research efforts has proven the effectiveness of separately considering the PwrRad% and AvEnrg% metrics for all design, analysis, and simulation purposes.

For HTA vehicles operating during the lightest winds (< several m/s), energy can be stored more efficiently by re-positioning the vehicle than by climbing or re-charging the Energy Storage System (ESS). Re-positioning upwind at night will not adversely affect energy storage because the vehicle stall speed is substantially greater than the light wind speed, by definition. Re-positioning during the daytime also will not adversely affect energy collection because light winds enable almost the full range of *Sun-tracking* flight patterns. Because LTA vehicles can operate at zero flight speed, however; the ability to position upwind at no additional cost to the energy system is not possible. Thus, maintaining on-site operations at a flight speed equal to the wind speed is usually the most efficient option for LTA vehicles.

During moderate to strong winds, re-positioning HTA vehicles upwind is an inefficient method to store energy. It is strongly limited by the vehicle performance and requires significant energy expenditure. Similar to upwind re-positioning, the energy necessary for recovery-to-site during periods of moderate to high winds is extremely high. Although prompt recovery-to-site might be desirable, the most efficient recovery strategies exploit off-site climbing and ESS re-charging as first steps toward recovery. Re-positioning and recovery-to-site depend strongly on the relative speed of the vehicle and wind, whether the vehicle is on-site or off-site, and whether it is day or night. Energy expenditure is therefore guided by operational strategies (decisions) derived from a few rules linking the vehicle performance and energy characteristics to the on-site radius, time of day, and atmospheric conditions during a time step. All of these input parameters can be modified by the user to define the various operational strategies.

3.1.4 Persistent and Recoverable Flight Patterns

The analysis model includes a mission-level utility to identify persistent and recoverable (i.e., station-keeping) flight patterns. The model is based on a mathematical representation of the vehicle and wind speed vectors during each time step for points within the site radius limits. A set of discrete outbound vectors is

generated by combining the wind speed vector with the range of possible flight speeds and headings according to user-specified intervals. Subsequent calculations provide a means to identify the return vectors which allow persistent out-and-back flight patterns. These important constrained patterns are called *recoverable flight patterns* and they are illustrated in Figure 3.
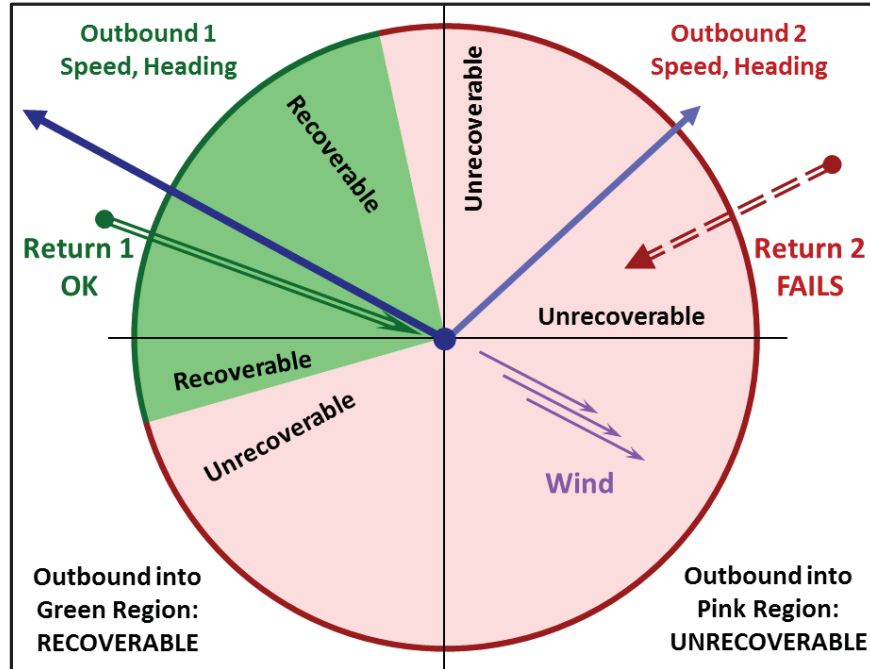
Figure 3. Recoverable flight patterns.

The methodology considers the possibility that a vehicle could depart upwind relative to the ground, against the wind vector and return by: 1) turning and flying downwind relative to the ground, assisted by the wind vector, or 2) maintaining an upwind heading and flying against the wind vector while drifting downwind relative to the ground. Given a specific recoverable flight pattern, it is possible to calculate the outbound flight time, the return flight time, and the relative vehicle-Earth-Sun orientations during the outbound and return segments. Combining recoverable flight patterns with solar energy collection utilities enables the unique capability to trade flight path vehicle power requirements and vehicle energy collection capabilities for each recoverable pattern. Only recoverable flight headings are evaluated by the SolFlyte analysis model when determining the optimal vehicle-Sun orientations for collecting energy.

3.1.5 Solar Energy Calculations

Determining the available solar energy flux at the operating altitude involves modeling external physics, solar array efficiencies, vehicle surface geometry, internal electronic efficiencies, vehicle-to-Sun orientations, and shadowing. The solar energy flux, including variations due to orbital parameters, time of day, time of year, flight altitude, and mission site latitude and longitude is calculated in SolFlyte using an algorithm developed from information provided on the Naval Observatory Astronomical Publication website:

http://aa.usno.navy.mil/faq/docs/Alt_Az.php   (accessed December, 2014).

The solar energy lost to atmospheric absorption is calculated at the operational altitude based on the simulated atmospheric conditions during the time step. The resulting attenuated solar energy flux is the maximum energy available for collection by a solar array oriented normal to the Sun. This section describes

9

the methods used to calculate the time-varying solar energy available for collection by solar arrays that are installed on a solar electric vehicle concept, at a generalized orientation to the Sun.

Solar Flux at the Vehicle Position

Calculating the relative orientations of the Sun to the vehicle solar arrays begins with calculating the Earth-to-Sun distance, and the solar altitude and azimuth at the given mission site and time. The values are used to calculate the solar energy flux and the solar incidence angle to each solar panel of the vehicle. Calculating these solar flux vector components in the Earth-based reference frame is relatively straightforward, but transforming the components to the vehicle flight reference frame and then to the installed arrays is substantially more complicated, particularly for general flight orientations. By assuming the vehicle flight orientation is level, the vehicle z-axis aligns with the Earth z-axis, thereby simplifying the coordinate transformation from the Earth to the vehicle. Calculating the solar flux vector components to the mounted solar arrays also requires a vector transformation from the vehicle reference frame to the array reference frame. This vector transformation is known from the design geometry and is implemented prior to the analysis by mathematically describing the array panel corner coordinates as an oriented array surface in the vehicle body axes. The parameters and an overview of several reference coordinate systems included in the solar flux vector calculations are illustrated in Figure 4.
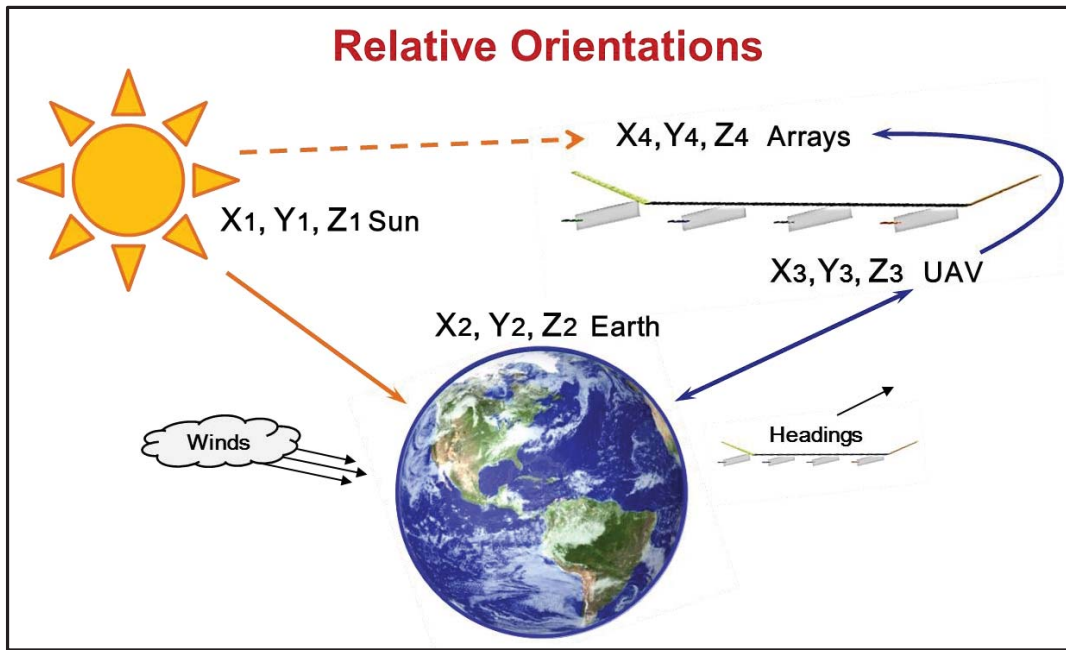
Figure 4. Solar orientation model.

Although the coordinate systems of the Sun, Earth, UAV, and arrays can be defined to simplify subsequent calculations, the coordinate transformations must also reflect the conventional use and orientation of these axes. For instance, the wind *blows from,* the vehicle *points towards,* and the flight *heads towards*, a direction measured clockwise from North = 0º. On the other hand, the solar azimuth is measured clockwise from East = 0º, as viewed from the Earth to the Sun, and the solar altitude never exceeds a magnitude of 90º. Within the reference frame of the trigonometric functions, angles are measured counter-clockwise from the + x-axis. Therefore, it was important to ensure all such conventions were smoothly integrated within and among the coordinate systems to avoid introducing phase, sign, or transformational errors. The directions and conventions used for defining some of these important orientations are illustrated in Figure 5.
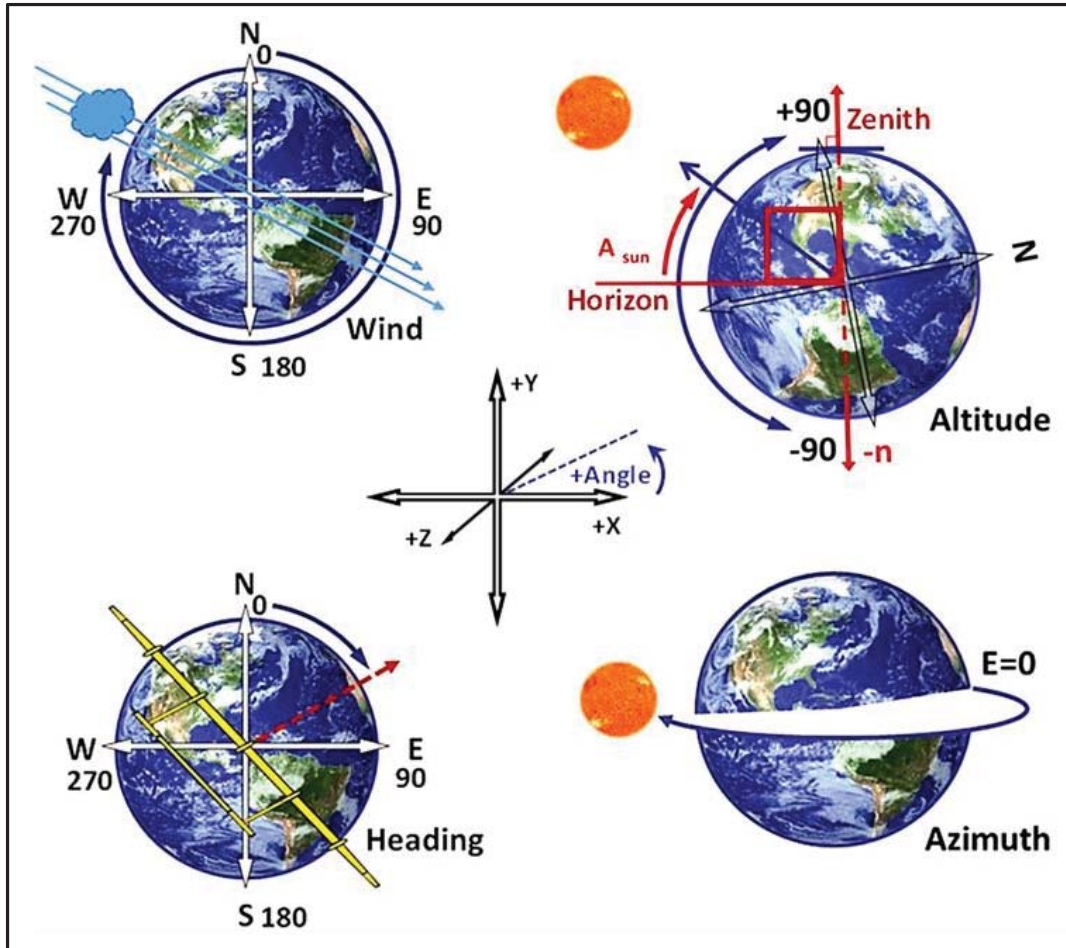
Figure 5. Angle definitions.

A reasonable inference might be that the level flight assumption restricts vehicle orientations and therefore eliminates the ability to model the effects of pitch or roll on solar energy collection. However, level flight does not restrict the range of possible Sun-to-Earth orientations or Sun-to-vehicle orientations. By referencing the vehicle body so the nose faces east and the right wing faces south, the Sun-to-Earth orientations could be transformed to the Sun-to-vehicle axes by adding the bank angle to the tabulated solar altitude. Although the entire simulation would include the constant bank angle offset, the method would be sound and useful for evaluating short periods of the mission. The approach would provide insight for assessing designs utilizing highly banked flight orientations at sunrise in order to quickly re-charge the ESS. The SolFlyte solar energy collection tables will be described in Section 3.1.6.

Solar Cell Transmission

The atmospheric attenuation factor decreases the available solar energy flux as a function of the mission altitude and the Sun-to-Earth incidence angle. The attenuated solar energy flux is then considered as the maximum available flux for that mission time step. Neglecting reflection at grazing incidence angles for an uncoated array surface, the solar energy illuminating a solar cell varies as the solar flux vector component normal to the solar cell. When functioning as a vehicle system however, protective and anti-reflective surface coatings modify the amount of solar energy transmitted onto the solar cell depending on the indices of refraction of the air, coatings, and solar cell surfaces. The variation of solar energy transmission with incidence angle, as used for this study, is shown as a red line in Figure 6.
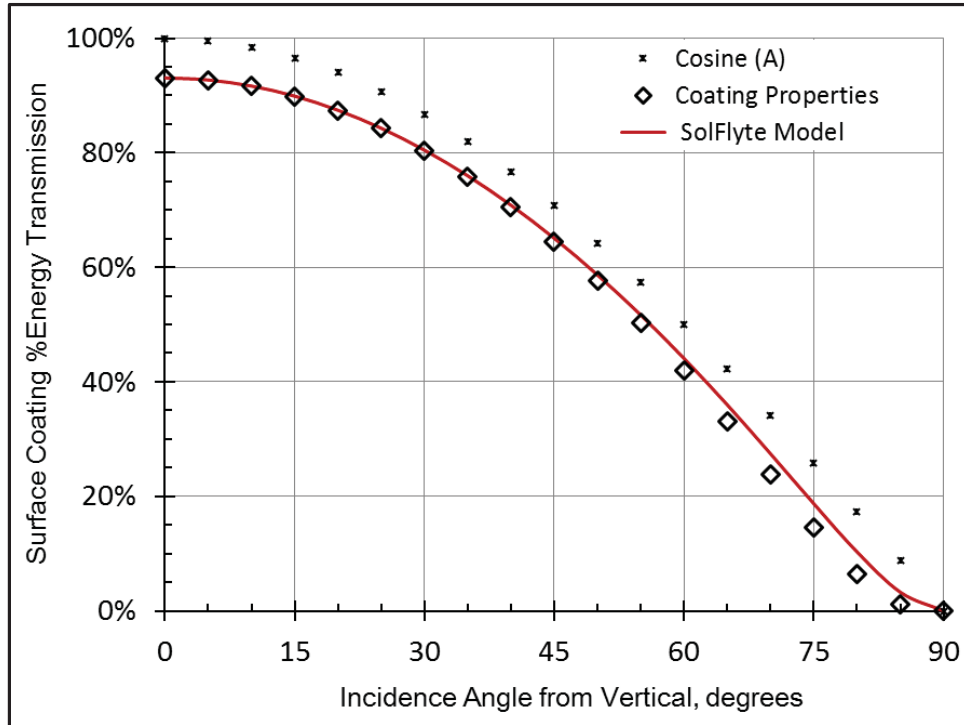
Figure 6. Solar cell array surface transmission model.

Solar Cell Efficiency and Energy Collection

A fraction of the solar energy transmitted to the solar array surface will be converted to electrical energy depending on the array temperature, cell array packing efficiency, and vehicle subsystem efficiencies. In addition, the nominal solar cell efficiency decreases with time due to cell degradation. Each of these parameters is considered when calculating the net energy availability during a particular mission time step.

3.1.6 SolFlyte Shadowing Assessment Utility

Background

In addition to the physics governing the solar energy available for illuminating an arbitrary solar array, the amount of solar energy collected and converted to electricity also depends on the vehicle geometry, solar array placement, shadows cast upon the solar arrays, and the Sun-to-vehicle orientation. To address these factors, the SolFlyte shadowing utility was developed as a mathematically rigorous tool for determining the effects of vehicle shadows on solar array energy collection for any Sun-to-vehicle orientation. The utility consists of two versions; a "single-point" orientation version used for initial analyses, and a "multi-point" orientation version used to generate tabulated output accessible during the SolFlyte mission simulation process. The multi-point version is executed once per vehicle configuration (i.e., the external geometry), for all Sun-to-vehicle orientations prior to use in the SolFlyte analysis model.

Vector and Geometry Modeling

The array geometry of each analysis vehicle configuration is approximated by a set of oriented panels with four co-planar corners in the vehicle body axis coordinate system. The (x,y,z) coordinates of these corners and the fraction of solar array coverage on each panel must be specified. For each panel, SolFlyte determines the mathematical vectors describing all edge orientations, spatial positions, and array areas. When executing the utility, opposite sides of each panel are modeled and output as two separate 1-sided panels, identified as facing toward or away from the Sun. The identification list provides feedback to ensure that the directionally oriented panels were properly defined in the vehicle coordinate system. Because the

energy transmission parameters vary with incidence angle, it is necessary to combine these factors with the calculations of the vehicle sunlit array area. Thus, the sunlit array area is best defined as an "effective energy collection area" which combines energy transmission and shadowing effects. Once the factors relating the Sun to the solar cell outer surface have been determined, the time-varying solar cell efficiency can be applied to calculate the electrical energy generated during the mission time step.

Figure 7 illustrates that shadows cast from separate panels upon an array target produce an overlapping shadow pattern (depicted as blue, red, and mixed areas). Each shadow pattern depends on the relative arrangement of every shadow-casting *cast* panel with respect to every other *cast* panel and the shadow *target* panel. Standard operations from vector calculus are used to determine the intersection points of sun rays cast through the four corner points of each cast panel to infinite planes containing each target panel. Each target panel region in the shade plane is considered as a series of strip vectors of differential width, segmented into bins, which, when integrated, yields the target panel area. The intersection points define oriented shadows associated with each cast panel within every infinite target plane facing toward the Sun, whether or not the shadow intersection points are within the array target region of the infinite target plane. All shadows in the solar array target region, are also parameterized as a series of strip vectors of differential width, segmented into bins. After intermediate calculations, the strip vectors can be summed to determine the shadowed area of each target array.

The shadow-to-target cast distances are also determined, measured from each shadow-casting corner to each infinite shadow-target plane, in the direction of the sunlight ray vector. Shadow darkness variations from atmospheric scattering can be related to these distances and used to weight the bins of each shadow strip vector. The shadowed area on each solar array, as weighted by the cumulative shadow strengths from the strip vectors of all cast panels, can be determined by summing all target panel shadow strips and bins. The shadowing effects of all panel combinations are integrated to obtain the vehicle solar array shadowing fraction at the specific vehicle-to-Sun orientation.
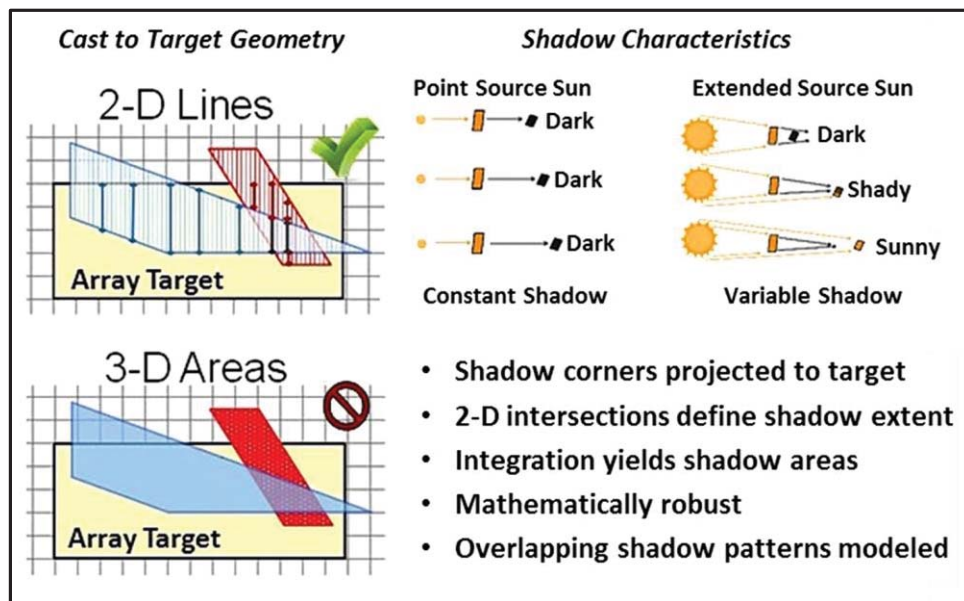
Figure 7. Shadowing geometry and features.

The Shadowing Assessment Utility can generate a table of normalized energy collection areas for the range of relative Sun-to-vehicle orientations between altitude angles of -10º to 90º and azimuth angles of 0º to 360º in 1º increments (36,461 unique orientations). Because execution time is approximately one second per orientation, sun tables are generated overnight in about 9 hours, only once per vehicle geometry.

During mission simulations, the SolFlyte analysis model extracts values from the sun tables almost instantaneously. As a result, SolFlyte mission simulations freely explore and identify energy rich flight headings and speeds. Figure 8 lists solar energy collection factors and illustrates example outputs of the single orientation version and multiple orientations version of the SolFlyte Shadowing Utility.

A final point of clarification is necessary to define the "Effective Normal Solar Array Collection Area". The term "Effective" indicates that the solar energy collection area contour values are normalized by the fraction of maximum viewable solar array area, not the total installed solar array area. For example, a double-sided array of area 10 m^2 per side would provide a maximum viewable area of 10 m^2, as viewed normal to the surface, neglecting all other energy collection efficiencies. The total installed solar array area would be 20 m^2. The maximum viewable solar array area of the HTA-450 utilized in this study is 260 m^2, as viewed from an orientation of 68° altitude, and at 90° and 270° azimuth, including all other energy collection efficiencies. The total installed solar array area is 450 m^2.
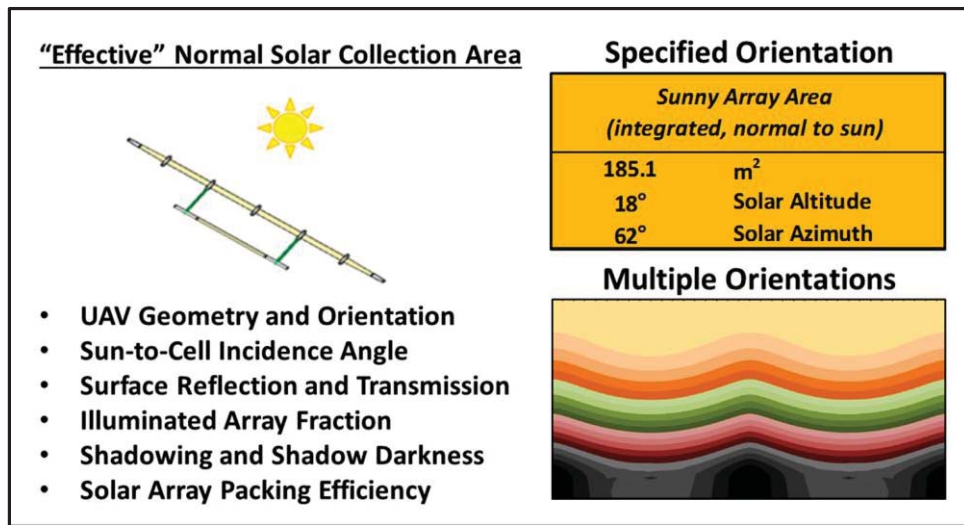
Figure 8. Features of the solar energy collection factor.

3.1.7 Climbing, Descending, and Altitude Variations

Climb and descent physics differ for HTA and LTA vehicle types. To account for these differences, SolFlyte incorporates two distinct models for simulating the altitude variations characteristic of HTA and LTA vehicles. During every time step, the analysis model integrates the specific climb and descent physics with all applicable influences already described in Sections 3.1.1 to 3.1.6.

Lighter-Than-Air

For LTA vehicles, the buoyancy force and neutral buoyancy level (density altitude) are calculated based on the atmospheric conditions, vehicle weight, volume, and lifting gas. At the start of a mission simulation, this information is used to determine the ascent rate and the ascent time to an initial operational density altitude. The operational density altitude is then mapped to two contiguous pressure altitudes of 100 mb, 70 mb, 50 mb, or 30 mb. The geometric altitude associated with the lower of the two selected pressures defines the upper altitude limit whereas the geometric altitude associated with the higher of the two selected pressures defines the lower altitude limit. To allow some flexibility to the LTA mission, it is assumed that the vehicle design enables operation within an altitude band defined by these two altitude limits. To decrease simulation times, the two remaining pressure altitude levels are eliminated from further consideration.

14

Heavier-Than-Air

HTA vehicles climb as a function of performance capabilities and atmospheric conditions, in accordance with operational rules. In the SolFlyte model, the vehicle operational rate-of-climb ceiling and the absolute ceiling are determined at the maximum power setting, based on an input rate of climb parameter and on a power-limited rate of climb equal to 0 m/s, respectively. Both ceiling parameters vary due to the atmospheric conditions at each time step, so the design ceiling, operational rate-of-climb ceiling, and absolute ceiling generally refer to different, varying altitudes, as shown in Figure 9.
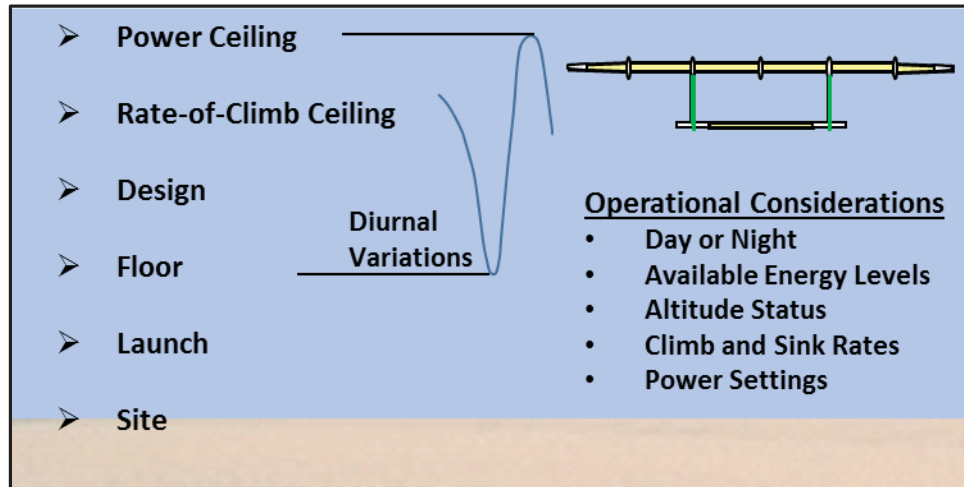
Figure 9. HTA altitude variations model.

Easily attainable potential energy can be stored by climbing during daytime periods when the usable solar power exceeds the vehicle power and energy replenishment requirements. The power setting and attainable climb rate are determined by considering operational parameters, vehicle performance, and the atmospheric conditions. If the operations are defined to enable daytime climbing for the purpose of storing potential energy, the climb power setting is utilized until the vehicle reaches the absolute ceiling, at which point the power setting is reset to a cruise power setting.

As power settings vary, the vehicle will continue to climb and descend near the absolute ceiling as solar flux levels permit. Sinking to recover potential energy is allowed only during simulated periods when the usable solar power is less than all vehicle power requirements, provided the vehicle is operating above the altitude floor. The attainable sink rate per time step is a function of the vehicle drag-to-lift ratio and the difference between the available and required power.

Storing and using altitude potential energy can significantly offset the demands on the energy storage and power systems, but the allocation of this energy depends on operational choices. To avoid influencing the simulation results as a consequence of pre-selected choices, the potential energy parameter is considered hypothetical and thus remains independent of all energy storage system and power system calculations. However, values of the hypothetical altitude and potential energy are listed as output parameters during each time step for consideration when interpreting results.

3.1.8 SolFlyte-LTA Analysis Model and Sizing Utility

ADAC was the product of a short-term effort within the ASAB during 2002 to provide some capability to design and analyze LTA UAV concepts, and to predict station-keeping capabilities during operations in time-variant winds (ref. 2). The ADAC architecture did not permit mission or analysis flexibility, and the user interface prevented straightforward assimilation with the envisioned modeling capabilities of 2010. However, elements of the sizing methodology, input and output selections, design considerations, and

mission simulation procedures were fundamentally sound and relevant to the new development efforts. The contrast of severe limitations and promising attributes within the ADAC analysis tool provided practical feedback to substantiate the approach needed to achieve the desired LTA design methodology and modeling capabilities.

The development of the SolFlyte-LTA model was an evolutionary process initiated with modifications to the functioning, completed SolFlyte-HTA model. Input parameter definitions within the SolFlyte-HTA "vehicle specifications" analysis component were revised, as needed, to accommodate differences associated with LTA vehicle concepts. Once the revisions were implemented, it was noted that many of the LTA specification parameters matched or shared common applicability to design parameters pertaining to airship design and analysis. To avoid redundancy, and to maintain consistency with the architecture of the SolFlyte-HTA process model, the common LTA vehicle specifications and the airship design capability were combined in one file and wrapped to create one analysis model component. Ultimately, the SolFlyte-LTA "vehicle specifications" component evolved to function as both the stand-alone LTA Sizing Utility and the means to insert LTA vehicle specifications to the analysis model. This characteristic adds sizing and parametric design capability to the SolFlyte-LTA model that is not currently available in the SolFlyte-HTA model.

The completed, enhanced lighter-than-air sizing utility developed for use in the SolFlyte-LTA model provides robust, general, rapid sizing estimates and iterative parametric design capability. Sizing input parameters and values are entered on the LTA Sizing Utility input spreadsheet. The required analysis parameter values are generated and saved separately and prior to executing SolFlyte-LTA. After the sizing is complete, the Excel file, input, and the output parameter values serve as the LTA specifications component in the SolFlyte-LTA analysis model. The SolFlyte-LTA model then accesses and links any sizing updates for use in subsequent simulations. The PHX ModelCenter® v9.0 interface allows users to over-write the LTA sizing outputs in order to execute the SolFlyte-LTA simulation model with vehicle specifications derived from other sources.

Extensive code modifications were required to capture the operational and performance differences of the LTA and HTA vehicles. Defining two consistent sets of operational rules for the LTA and HTA concepts was complicated by the unexpected implications of only a few factors. These factors include: possible LTA flight speeds = 0 m/s, required HTA flight speeds > stall speed, and determining the appropriate LTA operational speed during certain nighttime conditions.

3.2 Simulation Overview

The analyst controls the expression of the integrated SolFlyte modeling functionality by modifying various operational, mission, and vehicle input options. This section illustrates how certain inputs might influence the overall course of an analysis or the ability to complete the simulated mission objectives. A detailed description of all available analysis and specification input parameters is outside the scope of this study; however, information is available in the SolFlyte User's Guide.

3.2.1 Mission Operations

For SE-HALE UAV concepts, mission success depends on not only whether or not a vehicle has the capability to meet the mission objectives, but on how the capabilities of that vehicle are expended to meet the mission objectives. For instance, the simple choice of a late afternoon start time risks energy depletion and failure before the first sunrise of the mission; however, climbing to the operational altitude after an early morning launch would likely provide time to replenish the energy storage system before the first sunset. Similar strategies can involve exploiting such resources as vehicle-site positioning, altitude changes, flight headings in strong winds, and Sun-vehicle orientations in order to meet the mission objectives. Often,

capturing the gains afforded by a particular strategy is constrained by the physics of the vehicle performance, the instantaneous energy balance, or the environmental and solar conditions. Although the general approach to developing the SolFlyte operations model was to minimize "human derived" rules and to focus on identifying and applying physics-based operations constraints, both types of operational rules were implemented, and both influence simulation results.

All flight vehicle design concepts must include on-board systems that adequately meet the energy storage and power requirements of the vehicle and payload for the duration of the mission. In the particular realm of SE-HALE UAV analysis, the cyclical nature of energy collection, storage, and expenditure must be considered during the design of the vehicle, energy storage, and power systems. Furthermore, the instantaneous energy state of the SE-HALE UAV depends on temporal and environmental factors which vary during the mission, including: the flight latitude, time of year, time of day, wind speed, solar cell efficiency characteristics, and the Sun-to-vehicle orientation. These factors fundamentally alter the design and analysis of the vehicle, energy subsystems, and mission operations. Successfully integrating these factors to SolFlyte required identifying and creating unique analysis methodologies, metrics, and modeling parameters.

3.2.2 Vehicle Design and Analysis Applications

Energy Balancing
Figure 10 schematically illustrates how the ESS stored energy might vary during a brief 5-day mission. When assessing energy variations (the energy balance), the analyst must consider how to proceed when it has been determined that the vehicle concept has depleted all on-board energy reserves, shown in Figure 10 as beginning at time $t=t_1$. If the goal had been to determine the mission success or failure, the answer, of course, would be known. However, it there had been a need to ascertain the extent or duration of the failure, the analyst might wish to continue the analysis by implementing a strategy to account for energy reserve debts. Using this approach, the reserve energy peak to trough difference could be calculated and used to determine how much energy storage capacity would have been required to prevent the energy depletion. Additionally, in this case, the analyst would be challenged to describe the running energy status as either "available" or "depleted" during re-charging periods beginning at the time of maximum debt, $t=t_2$, and ending at the time of zero energy debt, $t=t_3$. The ambiguities suggested the need to clarify the analysis procedure by defining an *energy floor* input parameter.

SolFlyte enables users to set initial and minimum allowable on-board energy storage levels while also setting how the simulation proceeds if lower stored energy levels are calculated. For typical analysis applications, the energy floor value is set to *+0* to enforce a realistic minimum stored energy level of 0 kWh (energy debt = zero). Changing the energy floor value to *-1* removes the minimum energy limitation and permits an assessment of all energy storage levels less than 0 kWh. Selecting this option reveals peak-to-trough energy storage differences and facilitates substantial design insight regarding the energy storage system capacity. Additionally, the option permits the analysis and simulation to proceed on a hypothetical course, given the assumption that energy storage capacity will be increased, by an amount equal to the maximum accumulated energy debt, during subsequent design iterations. During each time step, the energy status parameter is set to a value of *+0* or *+1* to indicate energy depletion or availability, respectively. The AvEnrg% mission performance metric is the fraction of mission time steps when energy had been available divided by the total number of mission time steps.
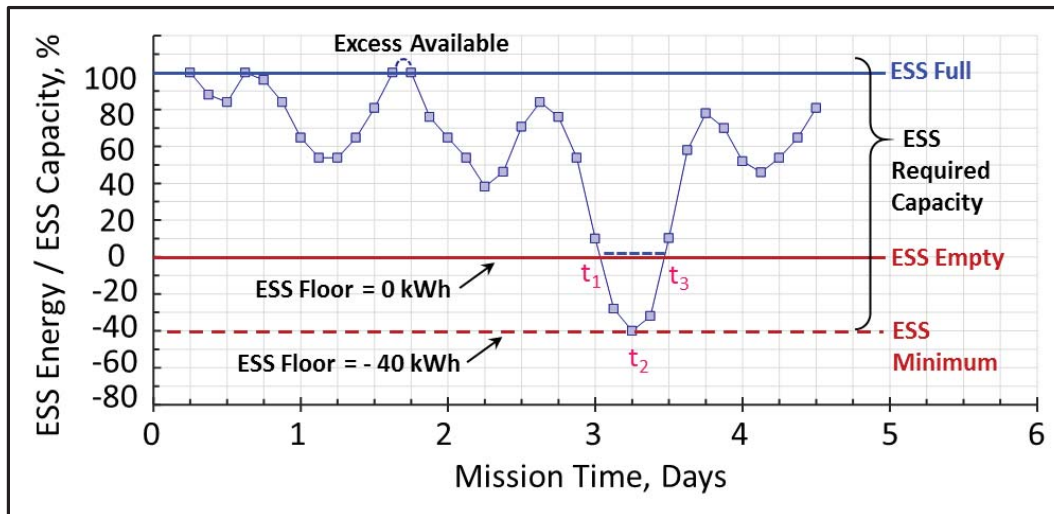
Figure 10. ESS stored energy variations.

LTA Vehicle Concepts: Special Considerations

For high speed wind conditions, airship design power and energy storage requirements can lead to size and weight growth factors that limit the practical feasibility of LTA concepts. The growth factors can be compounded during nighttime operations when available energy has been reduced by the round-trip efficiency of the energy storage system. A flexible set of input parameters was developed for sizing the power and energy storage systems. The power system is sized to ensure that the vehicle performance is capable of counteracting the highest anticipated site wind speeds, thereby enabling recoverable flight patterns. The *maximum vehicle speed*, and therefore the power system capability, is dependent on the mission site winds. The energy storage system is sized to ensure adequate energy availability for nighttime operations at the *energy usage speed* for a duration equal to the *energy usage time*, or for operations at the maximum speed for some other, likely shorter, duration. Similarly, the *energy collection time* is the specified period of time available for re-charging the ESS. The energy usage speed is generally set to a value less than the maximum speed to avoid vehicle sizes that exceed reasonable feasibility limits; and the energy usage time is generally set to the duration of the longest night at a mission site. The ESS sizing does depend on the maximum wind and vehicle speeds, but only as a consequence of providing available energy for powering the separately determined performance needs.

The modeling benefit of defining these three parameters is that the LTA power system design can be separated from the energy storage system design. Thus, the LTA vehicle concept power system is sized to satisfy the maximum speed requirement; whereas, the energy storage system capacity is sized as a function of the nighttime energy usage speed and energy usage time. By disentangling the power and energy system designs, the vehicle design concept is capable of speeds required for recoverable flight in the maximum wind conditions, whether or not energy would be available for powering all station-keeping operations. In other words, if the maximum wind speeds were encountered for an extended periods during a mission, the vehicle concept could possibly "run out of gas", thereby causing the overall mission performance parameter to indicate *mission failure*; however, the vehicle would retain the design speed capability. As SolFlyte separately tracks the status of both the energy storage system and the power system at every mission time step, the specific nature of an overall mission failure can be identified.

3.2.3 Output Description

At the completion of an analysis, the SolFlyte results are saved as "Excel.xlsm" files, named automatically according to the vehicle concept type, mission site name, the mission simulation start month. A real-time stamp indicating the completed analysis time is appended to the name to establish a unique and

organized pattern of results. For example, the "Spokane, March, 30-Day, HTA-450" case presented in this report was named, "*HTA-450_SPOKANE_Mar-09_8m18d10hr30min52s.xlsm.*" Each file lists parameters such as the vehicle speed and heading, and the atmospheric and solar conditions at each time step. The status of mission operational status parameters related to the energy storage system, operational altitude, and radial distance to the mission site are listed for each time step and for the entire mission.

The stored energy, altitude, and the vehicle-to-site distance are tracked during each simulated time step to calculate separate performance metrics during each simulated mission. The metrics are based on determining if the status of a given parameter would have enabled satisfactory operations during each time step. The summation of satisfactory operational times as a fraction of the mission duration provides insight to how individual parameters influence mission success or failure. For example, if direct or stored energy reserves were available during a given time step, the energy availability performance status would be credited *+1*. On the other hand, if the combined direct and stored energy reserves had been depleted during that time step, the energy availability status would not be credited (i.e., *+0*) and the overall mission performance would be set to *failed*. If energy had been available during four time steps and depleted during one time step, the energy availability summation as a fraction of all mission time steps would be *80%*, thus demonstrating the AvEnrg% calculation. Although status parameter values can switch between *+0* and *+1*, the overall mission performance flag cannot be reset once status parameter failure has been registered; however, the simulation will continue until the final time step is evaluated.

The values of the vehicle-to-site distance, the vehicle altitude and the energy availability status parameters can be summed to obtain an overall mission performance metric. Table 1 utilizes the AvEnrg% metric as an example of how the various inputs and mission status values are calculated and considered when assessing the overall mission performance. To illustrate, the "overall mission performance" and the "mission energy availability" both depend on the energy availability level at each time step, but they also depend on the "energy floor" parameter. If the energy floor input parameter had been set to *0*, and if the energy storage level were less than or equal to 0.0 kWh during the time step, the mission status and overall mission performance would be set to *failed* and the energy availability status would be set to *+0*. If the energy floor input parameter had been set to *+0* and the energy storage level were greater than 0.0 kWh during the time step, then the overall mission performance would remain *satisfactory* and the energy availability status would be set to *+1*. However, if the energy floor input parameter value was input as *-1*, the energy availability status would be *+0*, and the overall mission performance would remain *satisfactory*.

Table 1. Energy Floor and Energy Availability Metric, AvEnrg%

Time Step	Energy Floor	Energy Level	Energy Status	AvEnrg%	Mission Status	Mission Objective
1	0	225	+1	-	+1	-
2	0	100	+1	-	+1	-
3	0	-25	0	-	0	F
4	0	230	+1	-	+1	F
5--End	0	350	+1	-	+1	F
5	-	-	+4	80%	+4	Failed
Time Step	Energy Floor	Energy Level	Energy Status	AvEnrg%	Mission Status	Mission Objective
1	-1	225	+1	-	+1	-
2	-1	100	+1	-	+1	-
3	-1	-25	+1	-	+1	-
4	-1	230	+1	-	+1	-
5--End	-1	350	+1	-	+1	-
5	-	-	+5	100%	+5	Completed

Wind data measurement status indicators are listed during every mission time step to indicate the nature of the mission wind inputs during the specific mission simulation month and year. This factor provides essential feedback to the analyst for assessing the wind data quality, measurement gaps, and if the wind data input had caused operational anomalies. Other outputs listed during each time step include the time of day, solar orientation, atmospheric conditions, vehicle speed, heading, flight level, and the north/south and east/west radial distance components from the vehicle to the site.

4.0 Study Approach

SolFlyte was utilized to compare and contrast the LTA and HTA station-keeping capabilities during various missions. Assuming benign wind conditions, the LTA concepts have the advantage of buoyant lift and can perform station-keeping operations with little energy. A second advantage is that the shape and relatively large surface area of the LTA concepts offers plentiful space for mounting solar arrays at optimal orientations. However, as winds increase, drag increases sharply as the LTA vehicle speed counteracts the wind speed in order to achieve persistent station-keeping. Thus, the LTA flight power required and energy collection needs increase substantially.

The LTA drag increase is attributable to increased skin friction drag, profile drag, and a third factor peculiar to airships and balloons. The forward flight of an airship "pushes away" a mass of surrounding air, equal to the product of the atmospheric density and airship volume. The air momentum change is categorized as an "air mass" drag force that is dependent on the vehicle speed, fineness ratio, and volume. The air mass drag is a first-order consideration at moderate speeds and a dominant consideration at high speeds. Airship growth factors dependent on the air mass drag preclude designing SE-HALE airships capable of functioning at the maximum power during all conditions. Thus, realizing the operational design advantages of station-keeping airships, while also limiting the vehicle size, requires the ability to continuously adjust power settings as a function of the wind speed. These influences were combined with the previously described mission strategies and the vehicle performance and energy requirements.

In contrast, during any wind conditions, HTA vehicle concepts must always operate at forward velocities greater than the stall speed in order to maintain flight. Therefore, station-keeping capabilities are inherent to HTA vehicle concepts for wind speeds below the stall speed threshold. In such conditions, the energy (power) required to persistently operate on-site is equivalent to the energy (power) to maintain level flight. However, collecting the solar energy necessary to generate the required power is restricted by the total surface area and the limited orientations available for mounting solar arrays. Because of these fundamental differences between the LTA and HTA concepts, it is difficult to perform a direct comparison of station-keeping performance. However, by utilizing the SolFlyte-HTA and SolFlyte-LTA analysis tools, these disparate concepts could be sized and then flown in identical simulated environments, with reasonably consistent operational methodologies to provide equitable comparisons.

4.1 Mission Requirements

On-site operations were defined as operating within a radius of 36 km from a centrally located surveillance site, and for the HTA vehicle only, an upwind re-positioning limit, extending an additional 24 km, was defined and utilized as well. As discussed in Section 3.1.3, upwind re-positioning is not advantageous for LTA vehicles. The mission failure "cutoff radius" was set to 108 km for both the HTA and LTA vehicles. Weather forecasting could provide information to facilitate making critical choices during extreme conditions, but the SolFlyte operational rules assume that forecasts are not available.

All mission simulations examined 36 outbound flight headings ranging from 0º to 360º in 10º increments. Speed increments of 2.0 m/s were used to generate a set of outbound speeds ranging from the stall speed to the maximum speed for the HTA simulations and from 0.1 m/s to the maximum design speed for the LTA simulations. An array of outbound flight segment candidates was generated to include all possible combinations of these outbound flight headings and speeds. Each outbound flight segment was assessed to determine the existence of either one or two corresponding return flight segments enabling a recoverable flight pattern. Note that during the day, optimal flight patterns are the occasional consequence of increased power expenditures to enable faster flight that ultimately leads to greater net energy increases.

The flight time, Sun-vehicle-array orientations, and shadowing effects were also determined for the outbound and return segments of each recoverable flight pattern during each time simulated mission time step. The energy difference of the solar energy collected and the net operating energy consumed while completing both the outbound and return segments was also calculated. All net energy differences for all flight patterns were then evaluated to identify the most energy optimal flight pattern at the simulated time.

The set of operational assumptions shown in Table 2 provide a reference to ensure consistency when comparing the HTA and LTA concepts. The design altitude parameter was set to provide flexibility to the LTA mission for operating within a narrow altitude band defined by contiguous pressure altitude levels, or by density variations at the operating pressure altitude level. This assumption proved to be somewhat generous and will be discussed in the results section.

Table 2. Comparable Mission Operational Concept Assumptions

Parameter	HTA-450	LTA-1080	LTA-570	Units
On-Site Radius Limit	36	36	36	km
Off-Site Radius Limit	72	72	72	km
Mission Cutoff Radius	108	108	108	km
Upwind Re-position Limit	24	-	-	km
Modeled Heading Increment	10	10	10	degrees
Longest Nighttime	14.2	14.2	14.2	h

4.2 UAV Design Parameters and Assumptions

The design specifications of one HTA and two LTA concept vehicles were input to SolFlyte for analysis and assessment of mission station-keeping capabilities. As for the mission operational considerations, the HTA and LTA vehicle design assumptions were specified to be as consistent as possible. Selected design assumptions and values of the vehicle performance, propulsion, and ESS subsystems are shown in Table 3.

The most similar requirements for the HTA and LTA concepts included the payload specifications, subsystem efficiencies, and the operational radius limits. The payload definition was specified as either a distributed or single-point mass of 454 kg (1,000 lb) requiring 5 kW of continuous power. The electrolyzer and fuel cell efficiencies were assumed to be 85% and 80%, respectively, leading to an ESS round trip efficiency of 68%. The nominal solar cell efficiency was assumed to be 25%, and the propeller efficiency was assumed to be 82% at all conditions.

Table 3. Comparable HTA and LTA Design Concept Assumptions

Parameter	HTA-450	LTA-1080	LTA-570	Units
Solar Cell Efficiency	25.0	25.0	25.0	%
ESS Round Trip Efficiency	68.0	68.0	68.0	%
Energy Storage Capacity	500	1000	500	kWh
Payload Power (Continuous)	5.0	5.0	5.0	kW
Payload Mass	454.5	454.5	454.5	kg
Propeller Efficiency	82.0	82.0	82.0	%
Motor Efficiency	98.0	98.0	98.0	%
Motor Controller Efficiency	99.0	99.0	99.0	%
Wiring Efficiency	99.0	99.0	99.0	%
Design Altitude	16200	18500	18500	m
Design Density	0.1608	0.1099	0.1099	kg/m^3
Design Speed (LTA Energy Usage Speed)	36.0	20.0	20.0	m/s
Minimum Speed	31.7	0.1	0.1	m/s
Maximum Continuous Speed	40.6	36.0	32.0	m/s

The energy storage system was sized for a longest night of 14.2 hours to approximate mid-latitude winter solstice design conditions. For the HTA-450 concept, the energy storage capacity of 500 kWh enabled overnight operations at maximum power, requiring the regeneration system to fully replenish the ESS during the ensuing 9.8 hour day. For the LTA vehicle concepts, the reserve energy usage time was set to 14.2 hours to enable overnight operations at speeds of 16 m/s and 20 m/s for the LTA-570 and LTA-1080 concepts, respectively. Energy storage capacities of 500 kWh and 1000 kWh were designed for use on the LTA-570 and LTA-1080 concepts, respectively. The regeneration systems were both sized using the LTA Sizing Utility to fully replenish the ESS during the ensuing 9.8 hour day.

Other specifications include the HTA speed and altitude parameters, minimum or stall speeds, design speed, maximum speed, and design altitude. The values were determined as reasonable for this type of vehicle based upon previous studies, whereas the LTA speed parameters were derived from a parametric study detailed below in Section 4.4. The minimum speed of the LTA concepts was set to a small positive value of 0.1 m/s, reflecting the LTA ability to float in one place.

4.3 Heavier-Than-Air (HTA-450) Airplane Concept

Completing station-keeping objectives during an extended mission requires that the vehicle design concept includes a capability to continually generate the power required to meet payload, subsystem, and flight demands. Generating and supplying that power depends on maintaining available energy sources; for the HTA-450, these energy sources include direct solar, ESS reserves, or any combination of the two. The cyclical variations of solar energy on a daily and seasonal period and of ESS energy during depletion and replenishment periods require balancing the HTA-450 power usage and energy availability throughout the mission.

HTA Vehicle Concept: ESS Sizing

During the design and sizing phase of this study, the ESS capacity was sized to provide sufficient reserve energy for all mission operations at the design cruise speed, for the duration of the longest night at a latitude of approximately 35° N. On the other hand, the power generation and propulsion systems were designed to enable station-keeping capabilities in high altitude wind speeds up to about 40 m/s, regardless of energy availability. By specifying the design parameters in this way, the mission energy availability and on-site power capability could be assessed separately. For the relative comparisons desired for this study, the specified design capacity was marginal to ensure that energy reserves *could be* depleted in extreme

conditions, but would not be depleted in moderate conditions. The capacity was determined iteratively based on analyzing results of multiple simulations at various sites and times of year. The value remained constant thereafter. In actual practice, the energy storage system would be designed to ensure that the energy reserves *would not* be depleted during extreme conditions.

HTA Vehicle Concept: Array Sizing and Energy Collection

The SolFlyte shadowing assessment utility, discussed in Section 3.1.6, was utilized to determine the solar array area and solar array orientations required to replenish the ESS in a time equal to the shortest day at the mission site. Figure 11 shows a typical output plot of energy collection contours showing the percentage of effective solar array area as a function of Sun position. Orange and yellow regions of the contour plots indicate good energy collection orientations; whereas gray and black regions indicate poor energy collection orientations. The yellow areas on the vehicle top-view graphic in the figure indicate horizontally oriented solar arrays, and the green areas indicate vertically oriented solar arrays. Initially, the HTA-1b vehicle configuration was selected for this study after evaluating mission simulation results utilizing various HTA design iterations. The HTA variants were of similar size with modified vehicle and array geometry.

The energy collection objective is to size and orient the solar arrays to maximize energy collection at every Sun orientation, but clarifying how to meet that goal has not been possible. With the aid of solar energy collection contours generated by the SolFlyte Shadowing Assessment Utility, it is now possible to assess how vehicle geometry modifications will impact solar energy collection. For example, although the ESS capacity of the HTA-1b configuration was properly sized, the energy cycle did not quite close because the solar arrays could not fully replenish the system before night. Analysis of the energy collection contours indicated that selectively adding vertical array area to the outboard pylons and aft section of the tail boom would eliminate the HTA-1b energy collection deficit. Subsequent analyses confirmed this prediction and established the HTA-450 configuration as viable for the intended missions.

The HTA-450 energy collection contour plot is shown in Figure 12. The increased energy collection at low solar altitude angles is represented by the significant expansion of the red areas, highlighted by yellow circles near Sun directions of 90º and 270º. The second-lightest gray contours also expand at low solar altitudes compared those of Figure 11, and the two darkest gray areas decrease, as indicted by the sizes of the yellow arrows in each figure. As a reference to facilitate comparisons, white lines were added to both figures at Sun altitude angles of 5º and 20º. (Note that all concepts used in this study are designated by the concept type and the total solar array area. In this case, the HTA-450 is an airplane concept with a total solar array area of 450 m^2.)
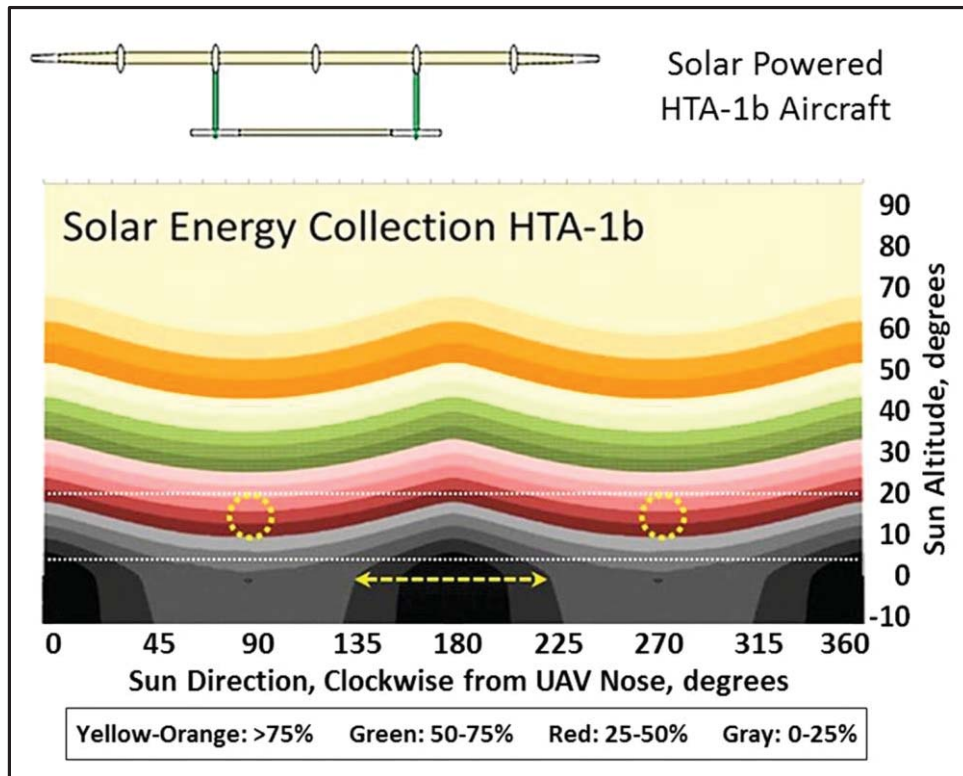
Figure 11. HTA-1b solar energy collection contours.
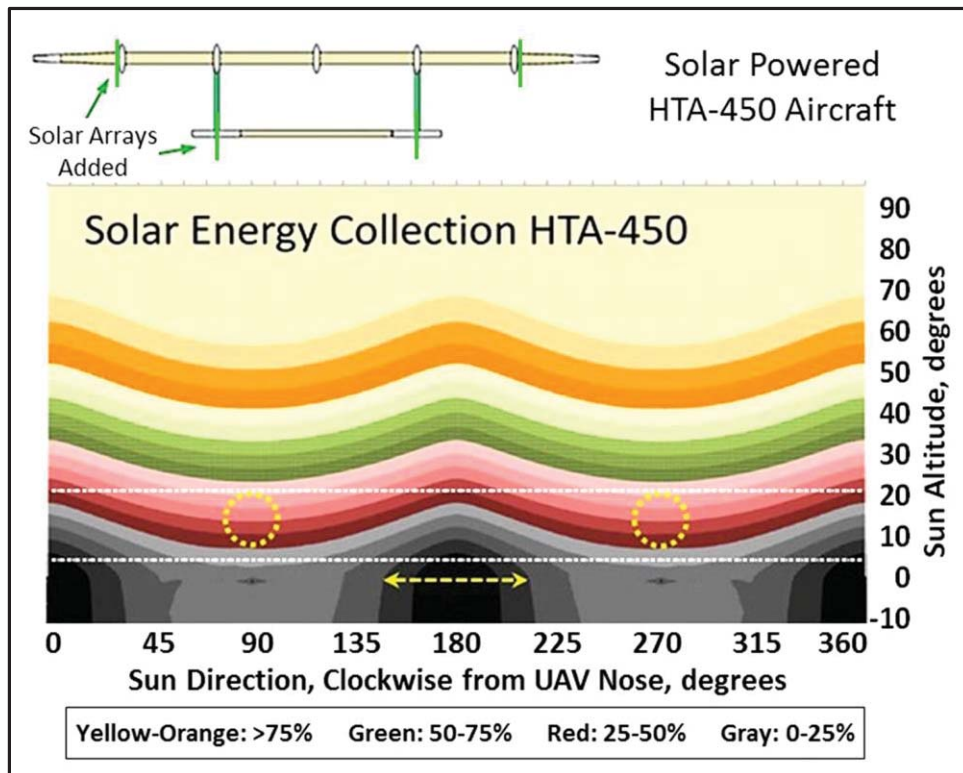
Figure 12. HTA-450 solar energy collection contours.

The previous example demonstrates that the energy collection contours provide meaningful assessment capabilities. However, the assessments described to this point include the inherent assumption that all energy collection orientations are equally weighted over the course of the mission. The implications of this assumption necessarily require that the operational time, and the mission criticality during that operational time (a weighted operational time), is equivalent for all points of the contoured solution space. To clarify, suppose that mission objectives would somehow not require operations if the Sun altitude were less than 20°. In such a case, the design modification leading to the HTA-450 concept might have been unnecessary.

It is possible to precisely identify optimal energy collection solutions which manifest operationally as energy optimal flight patterns. First, during the course of a day, the Sun follows a curvilinear path across the energy collection contour plot, as dictated by astronomical and geographical factors. This is depicted by the yellow dots in Figure 13. Second, wind speed increases relative to the vehicle speed will create unrecoverable flight patterns and operationally inaccessible regions of the energy contour plot. Furthermore, the individual "Sun" symbols located on the "Solar path" represent a specific time and Sun altitude angle at the mission site. As the Sun altitude angle is invariant at that instant in time, all possible Sun-vehicle-array orientations are therefore restricted to a single horizontal line passing through a selected "Sun" symbol. The recoverable flight headings are also restricted to that same horizontal line because of the alignment of the Earth and vehicle z-axes. Figure 13 (V_w= 0 m/s) and Figure 14 (V_w= 20 m/s) illustrate the results of a simulated 1-day test mission on September 21 at Santa Teresa, NM (~32° N) carried out utilizing the HTA-450 configuration. User-specified wind speeds were input to the simulation model for use throughout the mission at all flight altitudes. The blue dots in the figures indicate relative orientations from the vehicle to the Sun, whereas the red dots in the figures indicate the Earth-relative directional headings of the vehicle; both are measured counter-clockwise from the nose of the HTA-450.

HTA Vehicle Concept: Sun-Tracking Flight Orientations and Headings

The figures clearly show that energy-optimal Sun-tracking flight orientations trend toward 90° and 270°, corresponding to the right and left sides of the HTA-450 vehicle concept. As viewed within the Earth-based reference frame, the outbound and return flight headings would create a circular arc if plotted on a horizontally positioned compass (this arc would be circular only at dates near an equinox). The Sun-tracking flight orientations are shown to separate as wind speeds increase because the range of unrecoverable flight patterns increases with increasing wind speed. This effect forces deviations from the preferred 90° and 270° relative orientations. The recoverable outbound flight headings would resemble the green boundary arc of Figure 3. The return headings would create a similar arc, but it would be offset by approximately 180°, depending on the relative magnitude of the vehicle and wind speeds. If the entire pattern were then "filled-in", an asymmetric hourglass shape would be created.

HTA-450 Vehicle Concept Geometry and Specifications

The detailed structural and aerodynamic design of the vehicle was based primarily on modifications to proprietary data obtained from previous studies to obtain the final HTA-450 design concept. Key design specifications for the final HTA-450 configuration are shown in Table 4. Figure 15 shows top and isometric views of the HTA-450 concept, with solar array coverage identified by the darker regions. The solar arrays added to the HTA-1b configuration are visible on the most outboard pods and as increased coverage on both sides of each tail boom.
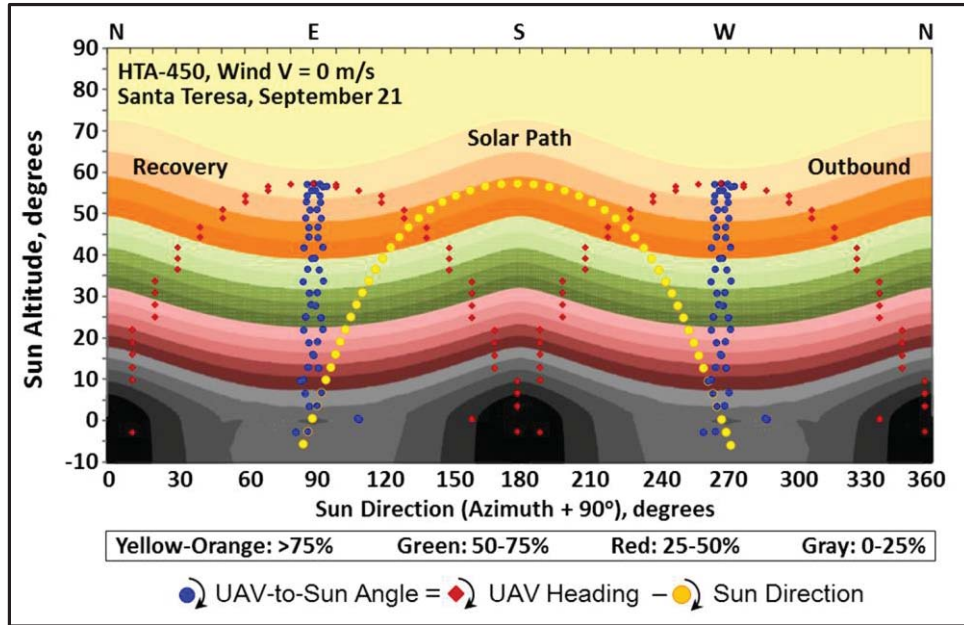
Figure 13. HTA-450 solar energy collection contours with Sun track and headings, wind=0 m/s.
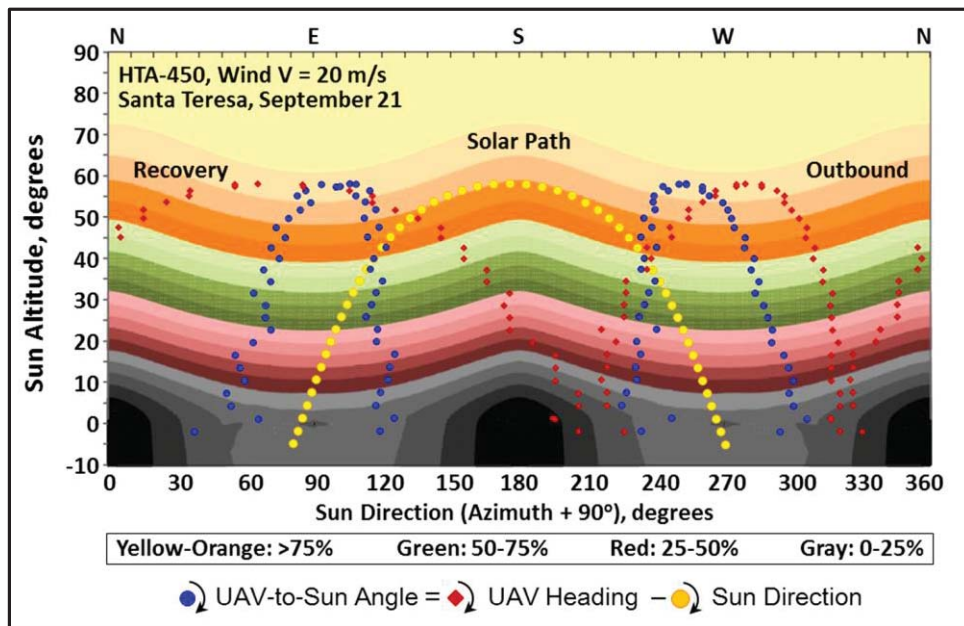

Figure 14. HTA-450 solar energy collection contours with Sun track and headings, wind=20 m/s.

To create a favorable span loading, the payload was assumed to consist of five components, each with a mass of 90.9 kg (200 lb) contained in five separate wing pods. Two outboard pods on each wing house both the payload and one of four regenerative fuel cell subsystems, but the centerline pod contains only the payload. The top view indicates that the wing pods are separated uniformly, by a distance of 22 m (72 ft). The vehicle OEW mass of 3285 kg plus the fuel cell reactant mass of 115 kg yields a TOGW mass of 3854 kg (8500 lb). The wingspan is 127 m (417 ft) and the total solar array area is 450 m^2. From the most outboard pods to the wing tips, a 14.5° dihedral angle was included to eliminate shadows on the vertical solar arrays mounted on the pods and facing toward the wing tips. At Sun-vehicle angles above 14.5°, a wider range of orientations becomes available for energy collection.

Table 4. Key HTA-450 Design Parameters

| Parameter	HTA-450	Units	Parameter	HTA-450	Units
Wing Span	127	m	Wing Loading a.)	11.5	kg / m^2
Projected Wing Span	126	m	Wing Loading b.)	2.35	lb / ft^2
Wing Chord	3	m	Number of Motors	4	-
Wing LE Sweep	0	degrees	Propeller Diameter	2.25	m
Wing Area	336	m^2	Pod / Nacelle Separation	22	m
Wing Aspect Ratio	47.8	-	Pod / Nacelle Length	8	m
Outboard Wing Section Span	19	m	Pod / Nacelle Diameter	1.5	m
Outboard Wing Section Dihedral	14.5	degrees	Boom Length	16.5	m
Operational Empty Weight	3285	kg	Boom Height	1.4	m
Payload Mass	454	kg	Horizontal Tail Span	55	m
Payload Power (continuous)	5	kW	Horizontal Tail Chord	2	m
Reactants (H2 and O2) Mass	115	kg	Horizontal Tail Area	79	m^2
Takeoff Gross Mass	3854	kg	Total Solar Array Area	450	m^2
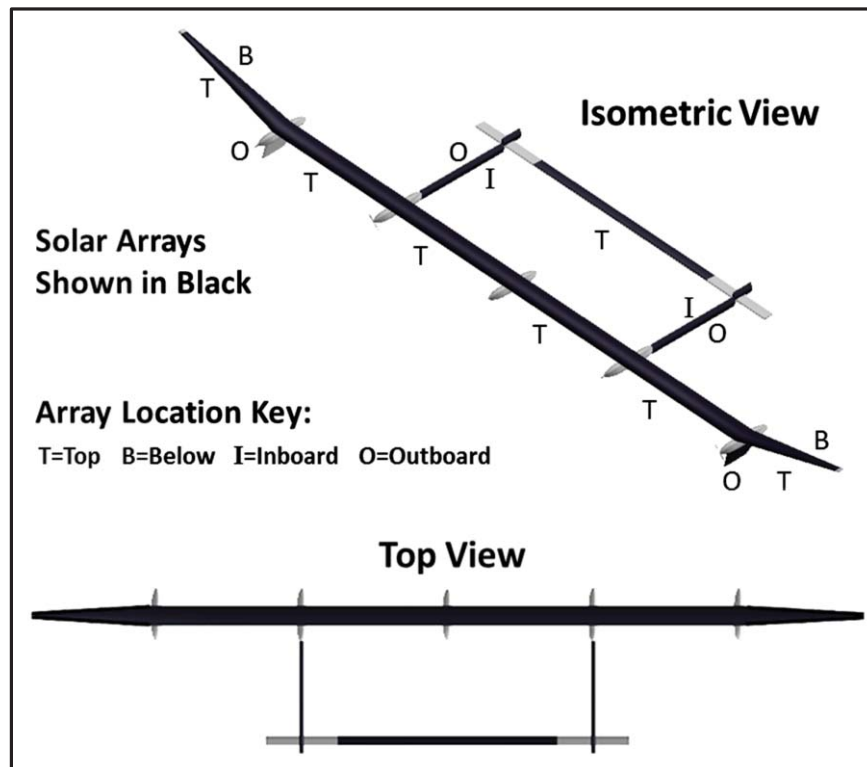
Figure 15. HTA-450 top and isometric views.

4.4 Lighter-Than-Air (LTA-1080 and LTA-570) Airship Concepts

The LTA Sizing Utility described in Section 3.1.8 was utilized to parametrically design two airship concepts. For all LTA cases presented in this study, it is assumed that the lifting gas is helium and the array mounting angle, defined later in this section, is 65°. To characterize the parametric design space of this study, the key design and size parameters of vehicle length, solar array area, power required, envelope volume, energy storage system capacity, and weight were plotted as a function of *maximum speed*, *energy*

usage speed, *energy usage time*, *and energy collection time*. The general approach to the design was initially constrained by the following assumptions and considerations:

- energy and power availability during winter solstice nighttime at mid-latitudes,
- volume feasibility of less than about 10^5 m^3,
- length similarity to the HTA wingspan of about 100 m,
- maximum design speed suitable for high wind speed conditions,
- and solar array area feasibility, estimated at < 1500 m^2.

A final consideration was that the general character of the LTA design concept would be reasonably comparable to the HTA design concept.

The top left graph of Figure 16 shows the relation between vehicle length and maximum speed. Airship length and volume increase dramatically with increasing speed as a result of the need to buoyantly lift heavier, more powerful propulsion and energy storage systems. The star indicates values associated with specifying a maximum design speed of 36 m/s; for this case, the resulting design length would be 135m. The resulting airship size and mass reveals the expense of specifying high speed performance capabilities for LTA design concepts.

The top middle graph of Figure 16 shows a similar relation between the vehicle volume and maximum speed. The maximum speed of 36 m/s corresponds to a design lifting gas volume of 72,500 m^3. Two comparisons provide insight to the dimensional scale of these parameters: the Goodyear Airship Eagle volume is 5740 m^3, the length is 59 m, and the width is 15m; and the Hindenburg volume was 212,000 m^3, the length was 245 m, and the width was 41 m. The bottom left graph shows that the required solar array area is 1080 m^2 for a maximum design speed of 36 m/s. The surface area of the LTA-1080 envelope is 10,900 m^2, so the required solar array area covers only 10% of the total vehicle area. The bottom middle and bottom right graphs show the relation of energy storage system capacity and power required to achieve the maximum vehicle speed. The top right graph shows that doubling the design maximum speed from 18 m/s to 36 m/s will roughly double the total weight, from a little less than 8,000 lb (the HTA TOGW = 8,500 lb) to almost 16,000 lb. The design TOGW for the LTA-1080 is 15,100 lb.
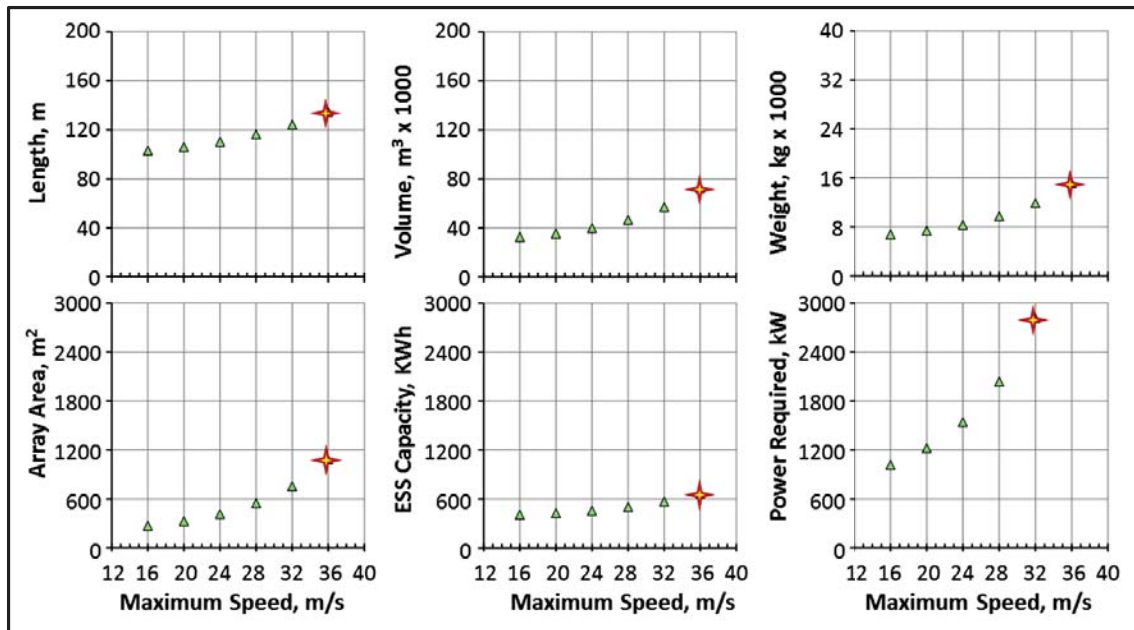

Figure 16. LTA-1080 parametric size variation as a function of maximum speed.

Figure 17 is similar to Figure 16, but the parameter sensitivities are shown as a function of stored energy usage speed instead of the maximum speed. Faster nighttime speeds ensure better on-site capability; however, as seen by the steep trends for all of the key vehicle parameters, additional nighttime speed can overwhelm other design considerations. The star shows the design points from specifying a 20 m/s energy usage speed capability for a nighttime duration of 14.2 hours. The sensitivity to the nighttime duration is also shown, with values of 12, 13, 14.2 and 15 hours. For this study, the energy usage time of 14.2 hours is approximately equal to the duration of the longest winter night at the mid-latitudes considered in this study. Figure 18 shows the sensitivity of key vehicle concept parameters to the complementary energy usage time. The sensitivities were evaluated at energy usage speeds of: 16 m/s, 20 m/s, 24 m/s, and 28 m/s.
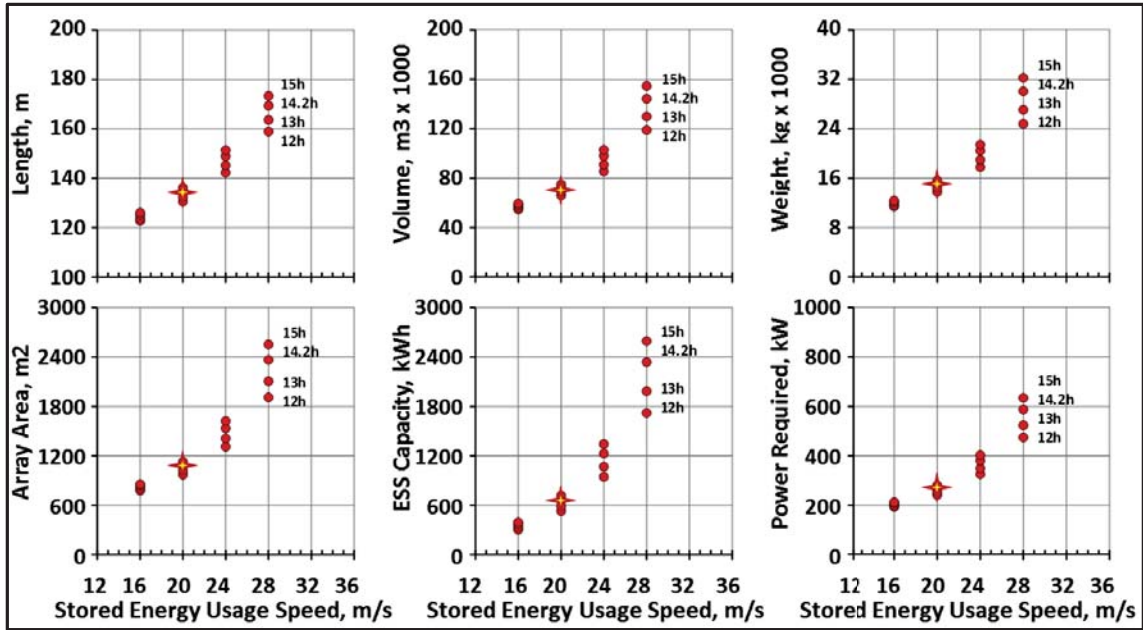

Figure 17. LTA-1080 parametric size variation as a function of energy usage speed.
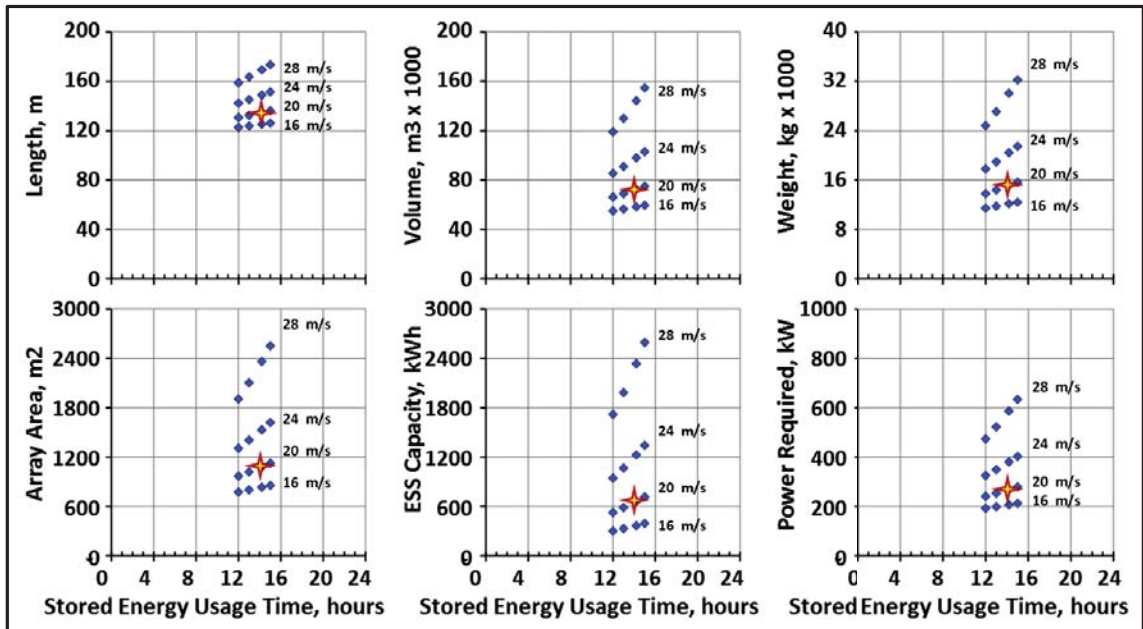

Figure 18. LTA-1080 parametric size variation as a function of energy usage time.

29

The final series of parametric sizing relationships is shown in Figure 19. The vehicle parameters are given as a function of solar energy collection time. A 9.8 hour shortest day was selected as the design point for determining the minimum time available to collect the energy needed to fully replenish the ESS.
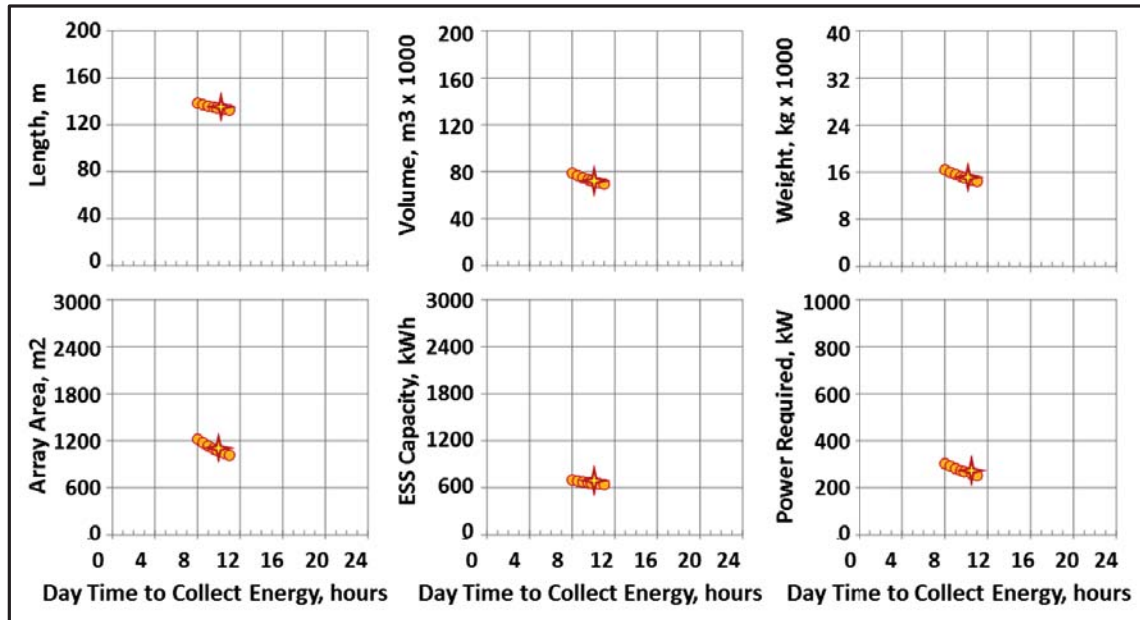

Figure 19. LTA-1080 parametric size variation as a function of solar energy collection time.

The internal volume afforded by LTA vehicle concepts provides structural options to design hard points for attaching concentrated mass. For this study, the payload, ESS, and propulsion subsystems were all considered to be concentrated masses attached to the bottom of the LTA vehicle concept. The payload was enclosed within a centerline pod, the ESS was enclosed within two pods located forward of the payload pod, and the propulsion subsystem, including propellers, was located aft of the payload pod. The relative sizes and general layout of the LTA-1080 vehicle, payload, ESS, and propulsion components are illustrated in the schematic bottom view shown in Figure 20. Two gray-colored propulsion pods and two gray-colored ESS pods frame one central green-colored payload pod. The payload pod smoothly tapers to a point at each end, has a length of 9.15 m, a width of 1.52 m, a height of 1.22 m, and an internal volume of 10.2 m^3.

Figure 20. LTA-1080 bottom view schematic: propulsion and payload (green) pods.

The shadowing utility in SolFlyte was also utilized during the LTA sizing process. One of the key design tasks was to find the optimal array placement on the vehicle. Although artist's conceptions of SE LTA vehicles usually depict solar arrays mounted to the top of the vehicle, such placement is suitable for a

limited variety of missions. For this study however, the 30-day missions were simulated during four seasons and the mission site latitudes range from about 30º N to 50º N. Thus, optimizing the solar array placement for a given mission site and season involves maximizing the total solar energy collection, while considering the daily and annual variations of the Sun-to-solar array orientation.

To identify the optimal solar array mounting angle, two strips of solar arrays were modeled at locations on the top of the vehicle, extending from the nose to the tail. For each analysis case, the strips were separated symmetrically by increments of 10º, as measured in a plane normal to the length axis, as viewed nose to tail. From this perspective, the array mounting angle is latitudinal, measured clockwise from horizontal to a terminal side which does not extend beyond the top of the vehicle. Thus, an array attached to the side of the vehicle, with an outwardly facing normal would be mounted at an angle of 0º, and an array attached to the top of the vehicle with an upwardly facing normal would be mounted at an angle of 90º.

Figure 21 schematically depicts how such solar array strips would appear as mounted on the LTA-1080 vehicle concept. Each array strip area is 540 m^2, for a total of 1080 m^2, mounted symmetrically on opposite sides of the vehicle. For shadowing analyses and simulation purposes, each array strip was modeled as seven distinct nose-to-tail panels. The panels were individually oriented to match the exterior slope of the vehicle at locations dictated by vehicle geometry and the solar array mounting angle. Seven similar vehicle configurations, characterized by array mounting angles of 30º, 50º, 60º, 65º, 70º, 80º, and 90º, were assessed to determine the best array mounting angle for energy collection. To provide insight to the design methodology, and to produce a single LTA design, Santa Teresa, NM (32º N) was utilized as a representative design site.
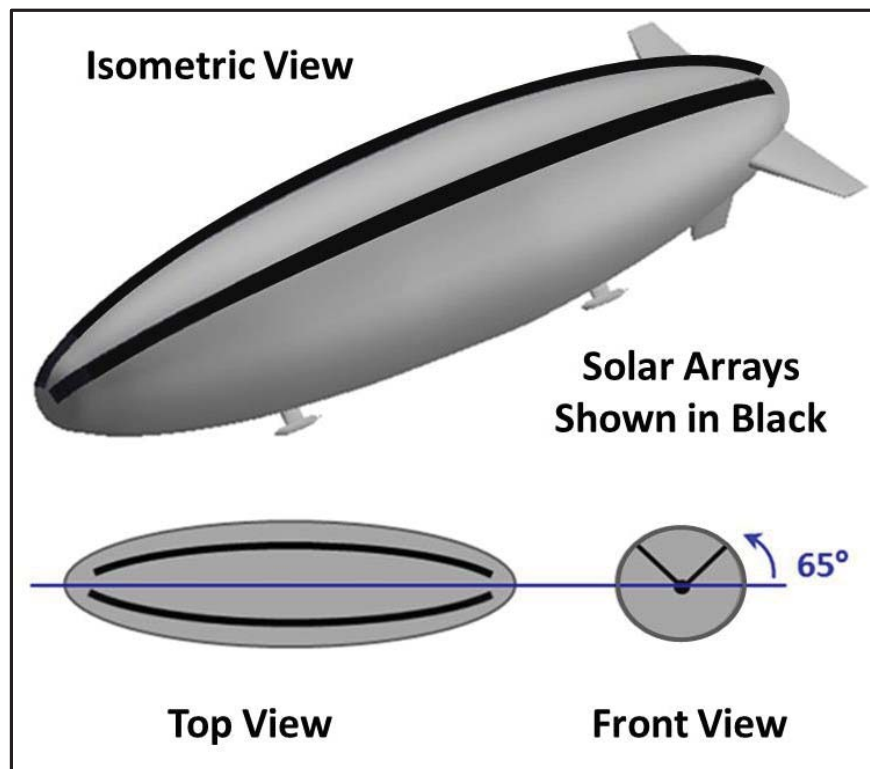

Figure 21. LTA-1080 isometric, top, and front views.

For most orientations, the LTA vehicle shape and the solar array placement shown in Figure 21 will allow simultaneous illumination of both array strips. The solar energy collection charts resulting from this arrangement are shown beginning with Figure 22 and ending with Figure 29. These figures were utilized

as a design tool for identifying and selecting optimal solar array mounting angles for the LTA vehicle concepts of this study. From left to right, at the top of each figure is the solar energy collection pattern for the side facing towards the Sun, for the side facing away from the Sun, and for both sides combined, each non-dimensionalized by the array area of one side. For the 90° case, the third contour is simply double the energy collection capability of each side. The large contour plot at the base of the figure is similar to the third plot, but the contours are non-dimensionalized by the array area of the entire vehicle. For the 90° case, the non-dimensional energy collection indicated by the fourth plot is equivalent to either side separately. The fourth figure is used as the basis for determining the energy collection efficiency within SolFlyte.

As the mounting angle is decreased, the contour patterns of the two strips combine to create substantially different patterns, and it is clear that a particular mounting angle would provide optimal energy collection for a given mission. Figures 30, 31, and 32 indicate the relative magnitudes of these variations referenced to different parts of the day during the months of March, September, and December, respectively. The advantages of the various mounting angles is evident for different times of the day as a result of the solar altitude angle. The inset shows a comparison of the relative magnitude of these advantages. Early and late day cumulative energy collection is indicated as a blue line and the mid-day cumulative energy collection is indicated as a red line. Finally, both lines of the inset plots were summed separately for the months of March, September, and December and are illustrated in Figure 33.

Figure 33 indicates the existence of an optimal mounting angle of approximately 50°, but the selection of the mounting angle requires evaluation of the particular mission requirements. For example, if the vehicle were used to carry out missions during December at a northern latitude, specifying a low solar array mount angle would improve energy collection. However, if the vehicle design maximum speed enabled operations during only spring, summer, and fall wind conditions, collecting additional energy during December would be unnecessary because the vehicle would be blown off-site. A low mounting angle might reduce energy collection and compromise the ability to carry out missions during other parts of the year. SolFlyte provides the modeling capabilities to carry out these necessary design trades.
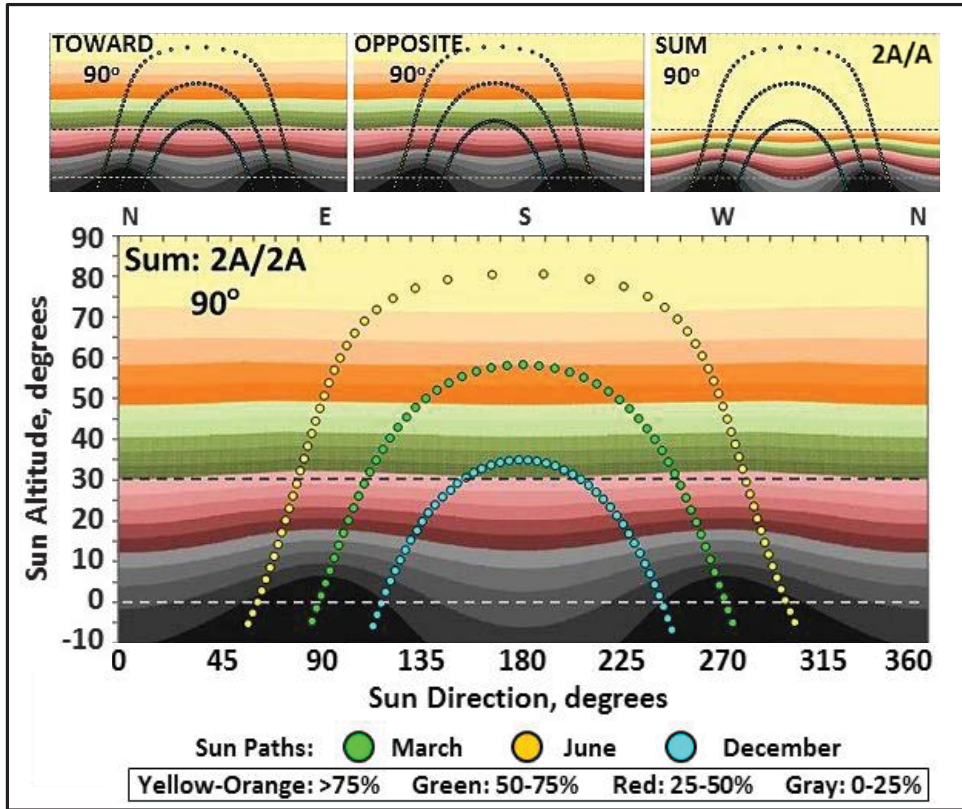
Figure 22. LTA solar energy collection contours: Santa Teresa, array mount angle = 90°.
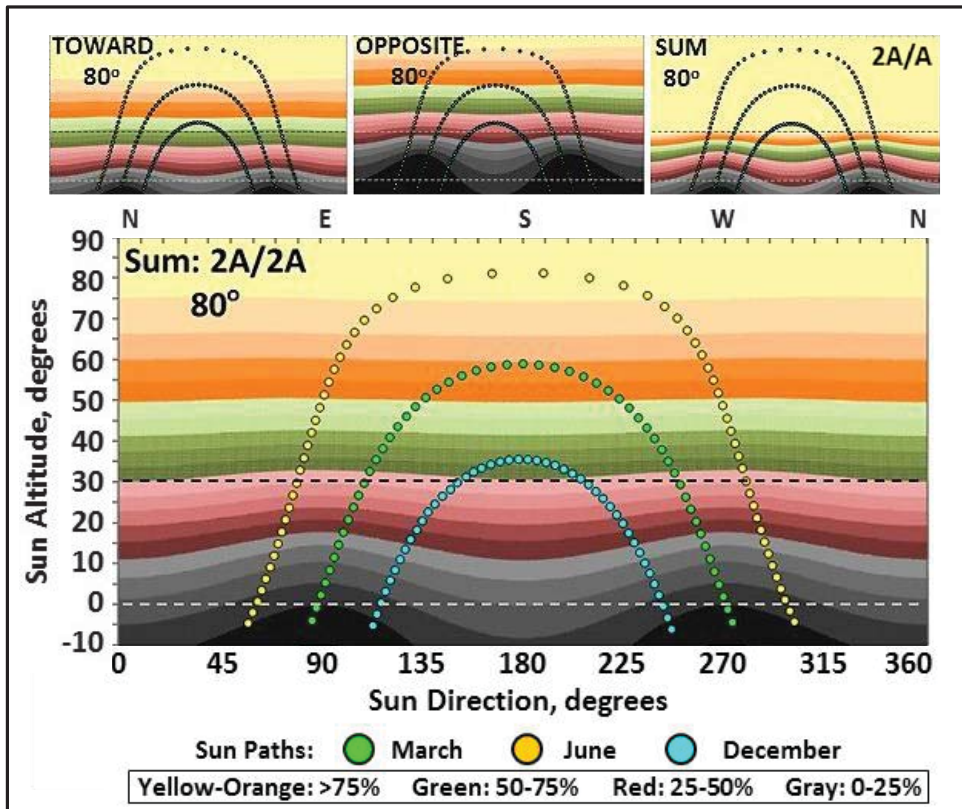
Figure 23. LTA solar energy collection contours: Santa Teresa, array mount angle = 80°.
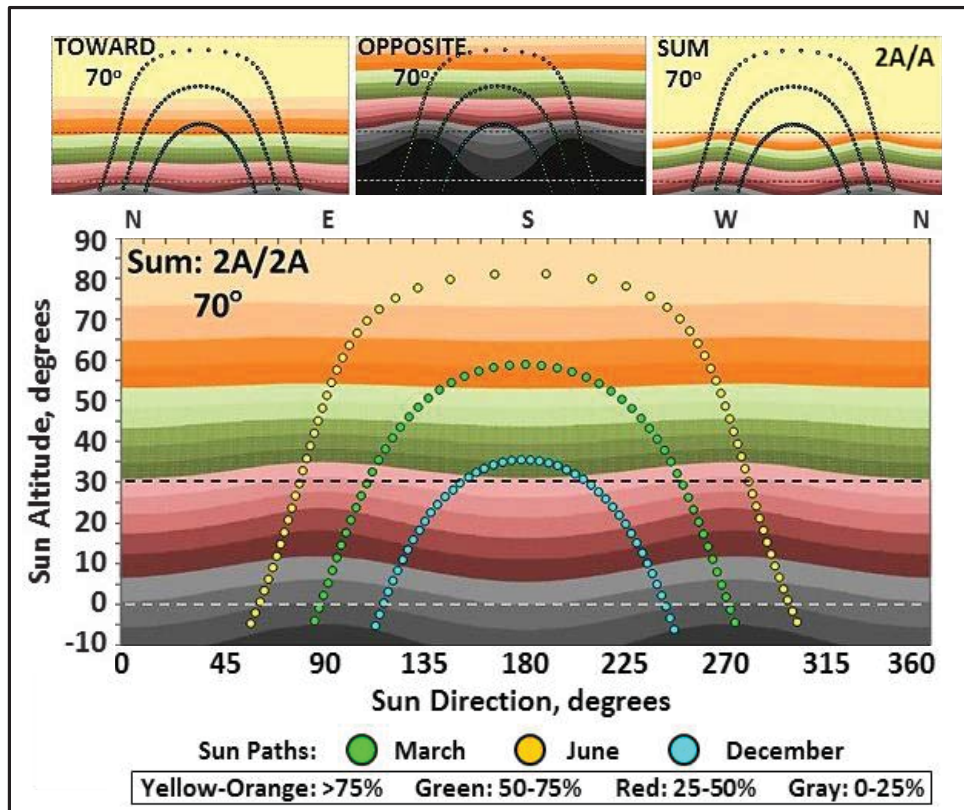
Figure 24. LTA solar energy collection contours: Santa Teresa, array mount angle = 70°.
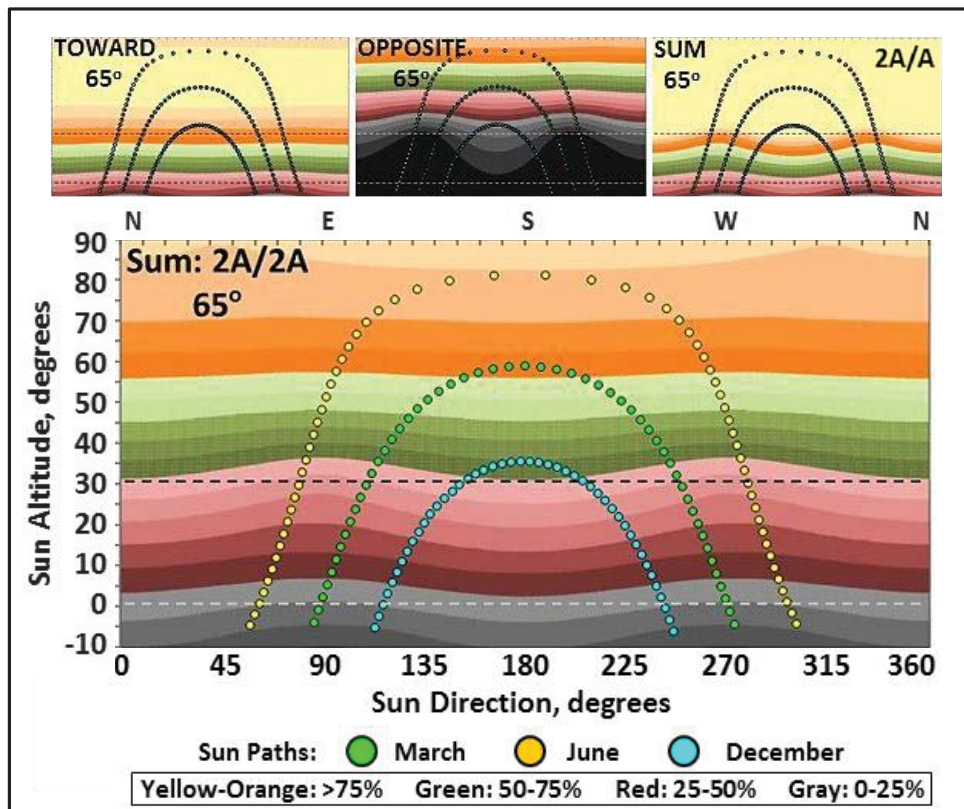
Figure 25. LTA solar energy collection contours: Santa Teresa, array mount angle = 65°.
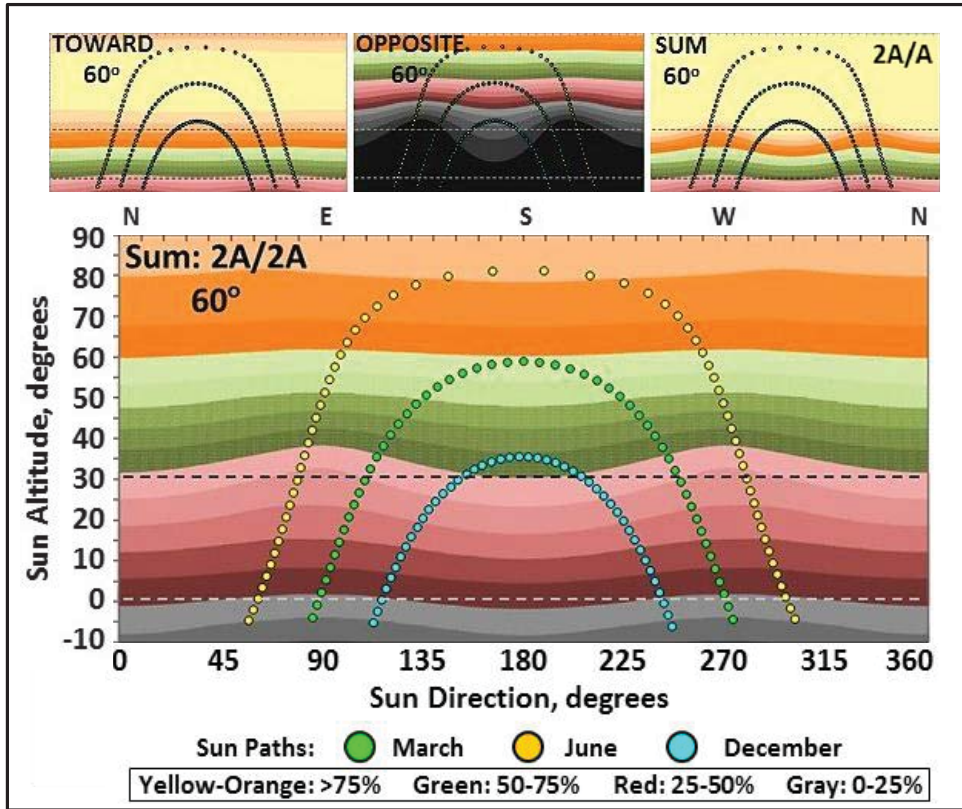
Figure 26. LTA solar energy collection contours: Santa Teresa, array mount angle = 60°.
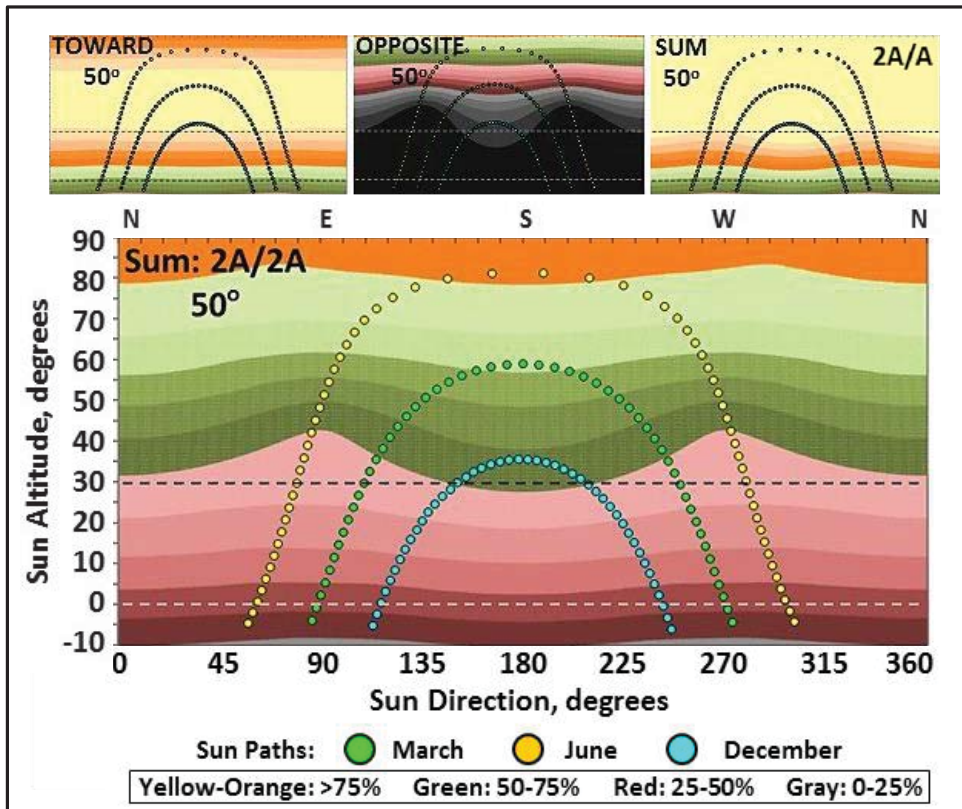

Figure 27. LTA solar energy collection contours: Santa Teresa, array mount angle = 50°.
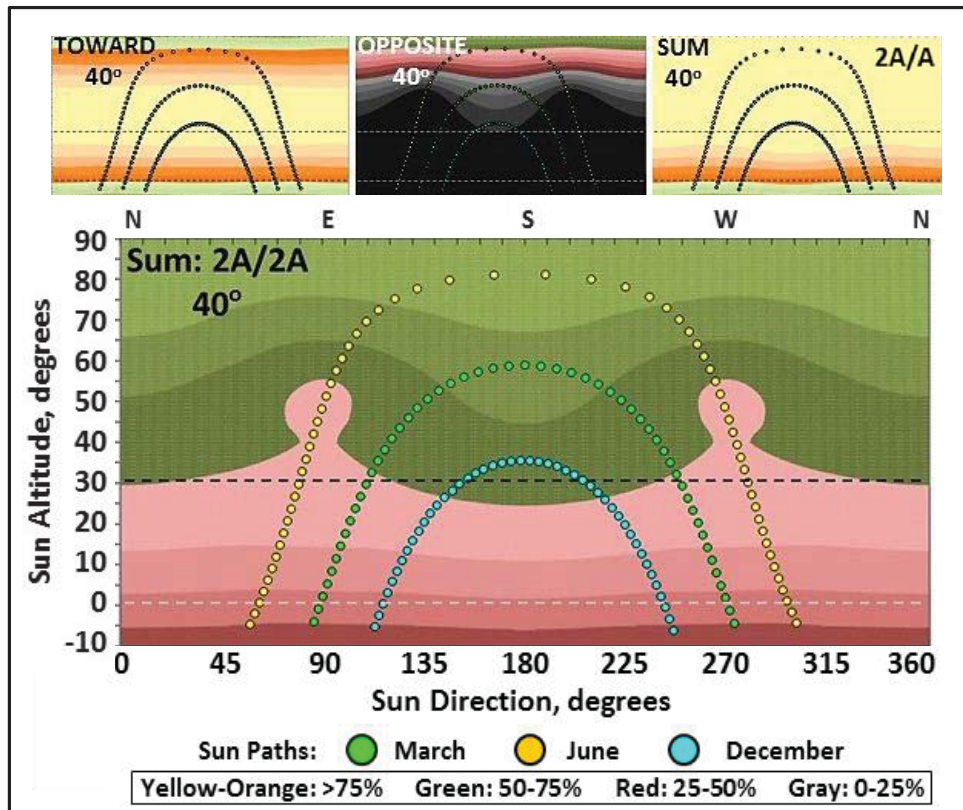
Figure 28. LTA solar energy collection contours: Santa Teresa, array mount angle = 40°.
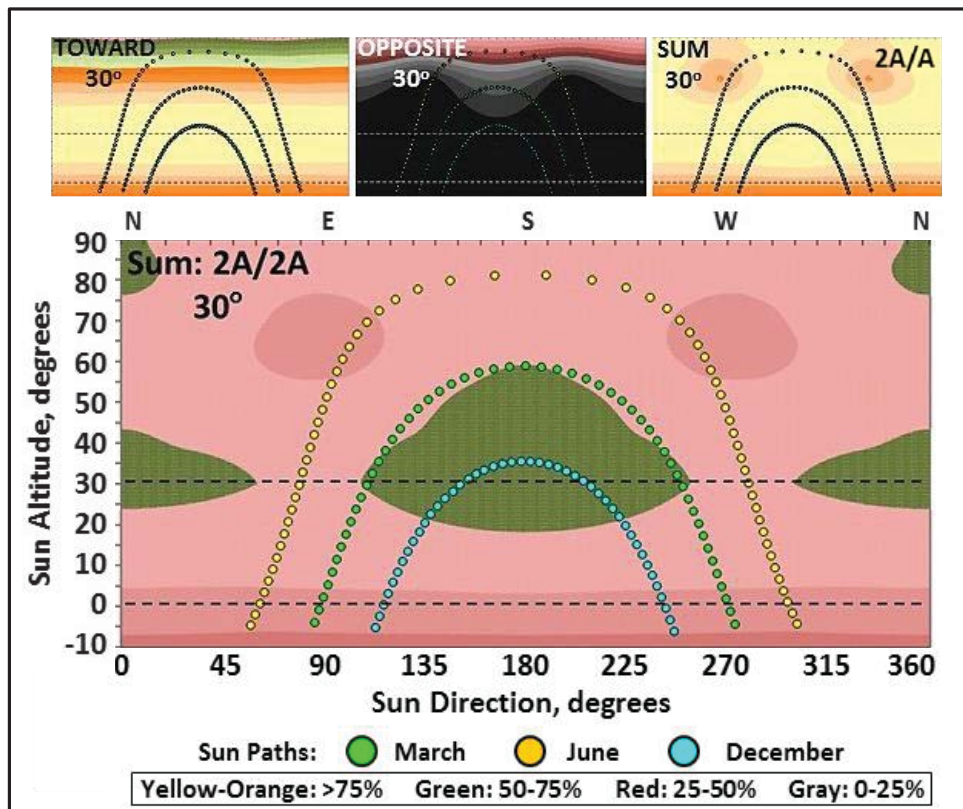
Figure 29. LTA solar energy collection contours: Santa Teresa, array mount angle = 30°.
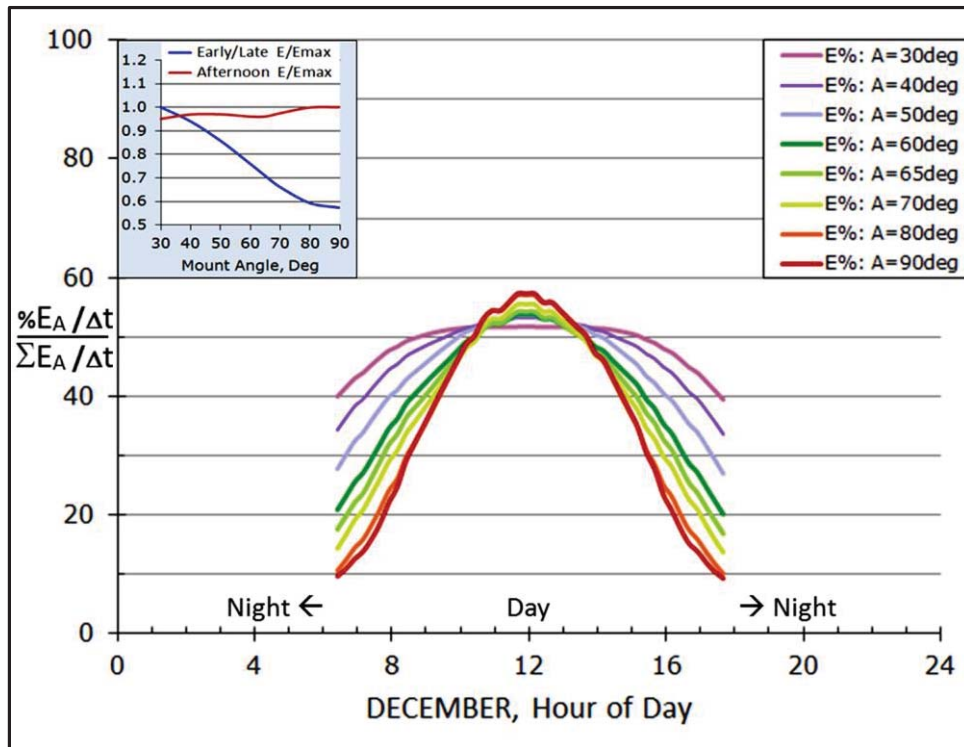
Figure 30. LTA normalized solar energy collection: Santa Teresa, December 21.
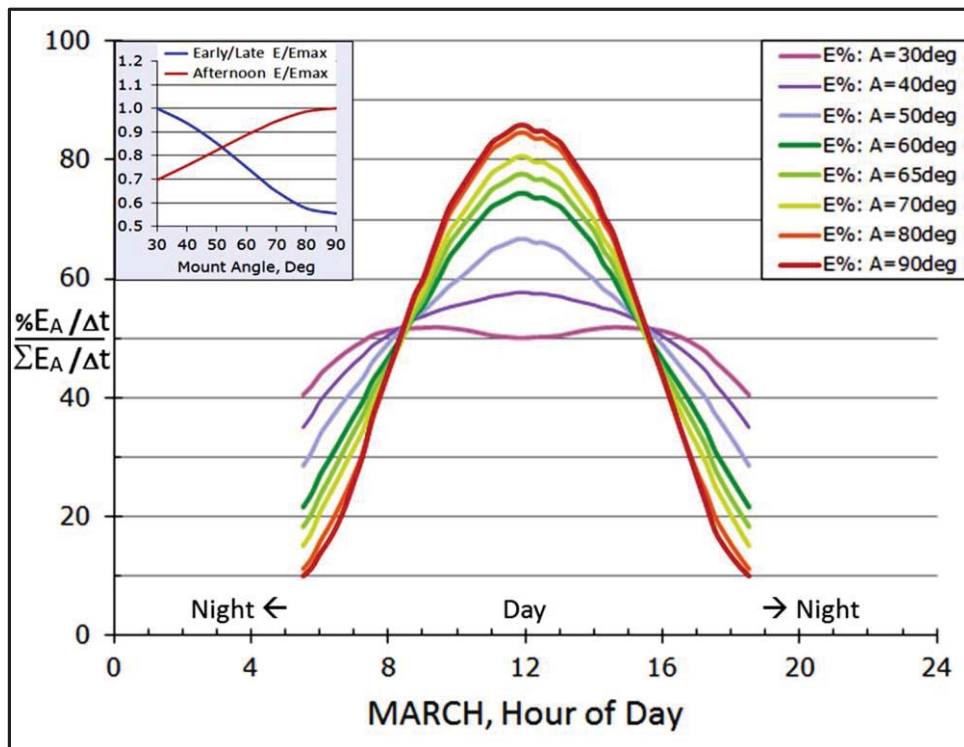
Figure 31. LTA normalized solar energy collection: Santa Teresa, March 21.
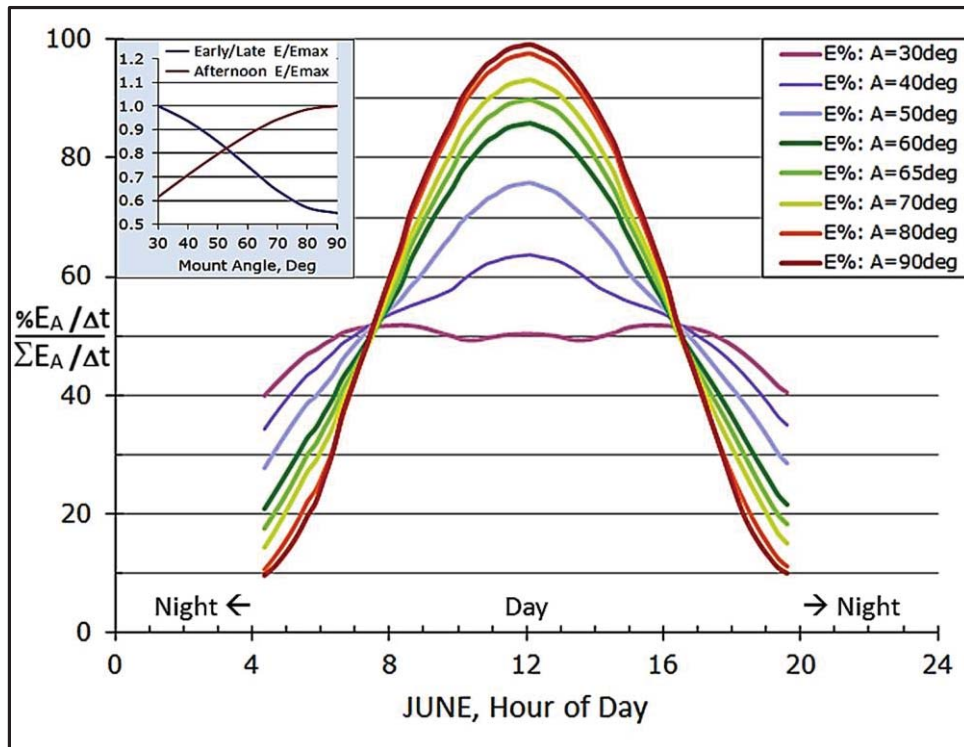
Figure 32. LTA normalized solar energy collection: Santa Teresa, June 21.
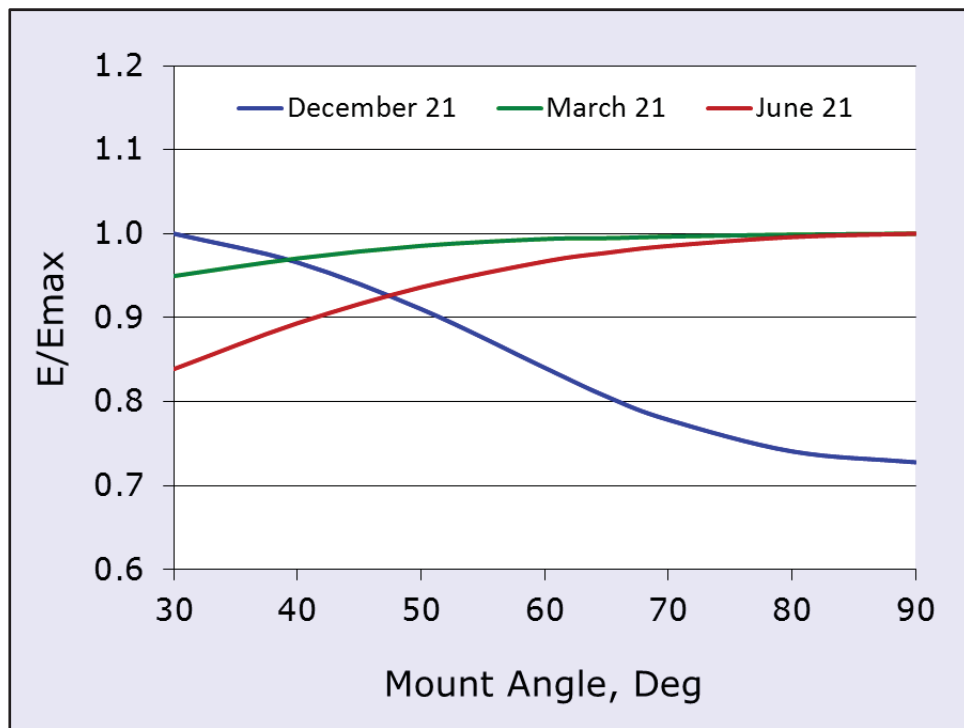
Figure 33. LTA time-integrated normalized solar energy collection: Santa Teresa.

Using the energy contours as a guide, both of the LTA concepts of this study utilized a moderate solar array mounting angle of 65° above the horizontal plane. At the completion of the LTA-1080 design, a

smaller LTA vehicle was designed. The LTA-1080 had been designed to provide mission performance capabilities similar to the HTA concept. To achieve the required performance, the size and weight of the LTA-1080 significantly exceeded the size and weight of the HTA-450. To enrich the overall comparison objectives of this study, the LTA-570 concept vehicle was designed to provide sizing similarities to the HTA concept; while the resulting mission performance capabilities were accepted as consequential. The modifications therefore diminished the LTA-570 performance and station-keeping capabilities relative to the LTA-1080.

To meet the LTA-570 size objective, the maximum design speed was reduced to 32 m/s, and the stored energy usage speed was reduced to 16 m/s. Both speeds are 4 m/s slower than the corresponding speeds of the LTA-1080; but, these relatively small speed differences led to the significant size and weight reductions evident in the LTA-570 design. The LTA-570 mass is 4318 kg, and the total solar array area is 570 m². The solar energy contours of the geometrically identical, but smaller-scale LTA-570, are identical to the HTA-1080 vehicle, within a constant value dependent on the total solar array area. Note that such scaling is possible only for conic geometry, as self-shadowing cannot be scaled for a generalized vehicle. Table 5 lists key parameters for the LTA-570, and the LTA-1080 designs.

Table 5. Key LTA-570 and LTA-1080 Design Parameters

Parameter	LTA-1080	LTA-570	Units
Design Lifting Gas Volume	72500	45700	m^3
Hull Envelope Area	10900	8000	m^2
Maximum Skin Thickness	0.1524	0.1524	mm
Total Solar Array Area	1080	570	m^2
Solar Array Mount Angle	65	65	degrees
Vehicle Length	135	115	m
Vehicle Maximum Width	32	28	m
Vehicle Maximum Height	37	32	m
Total Power Required	269	142	kW
Operational Empty Weight	6250	3790	kg
Payload Mass	454	454	kg
Payload Power (continuous)	5	5	kW
Reactants (H2 and O2) Mass	150	73	kg
Energy Storage Capacity	1000	500	kWh
Total Vehicle Mass	6854	4317	kg
Number of Motors	4	4	-
Propeller Diameter	2.25	2.25	m

Figure 34 is a scaled top-view showing the relative sizes of the vehicle concepts and the aircraft hangar facility at NASA Langley Research Center. The wingspan of the HTA concept and the lengths of both LTA concepts exceed the width and depth of the hangar; however, the diagonal length of the hangar floor is about 125 m, somewhat longer than the LTA-540 length and about equal to the HTA-450 wingspan. Figure 35 provides a scaled side-view perspective of the LTA-1080, the same hangar facility, and a variety of other aircraft. This view indicates that neither airship concept would fit inside the hanger; as the height of the LTA-540 and the height of the LTA-1080 height exceed the height of the hangar roof by 7 m and 12 m, respectively. Because the height of the HTA-450 would not prohibit entry to the hangar, it is feasible that facilities of this size might accommodate appropriately configured HTA concepts.
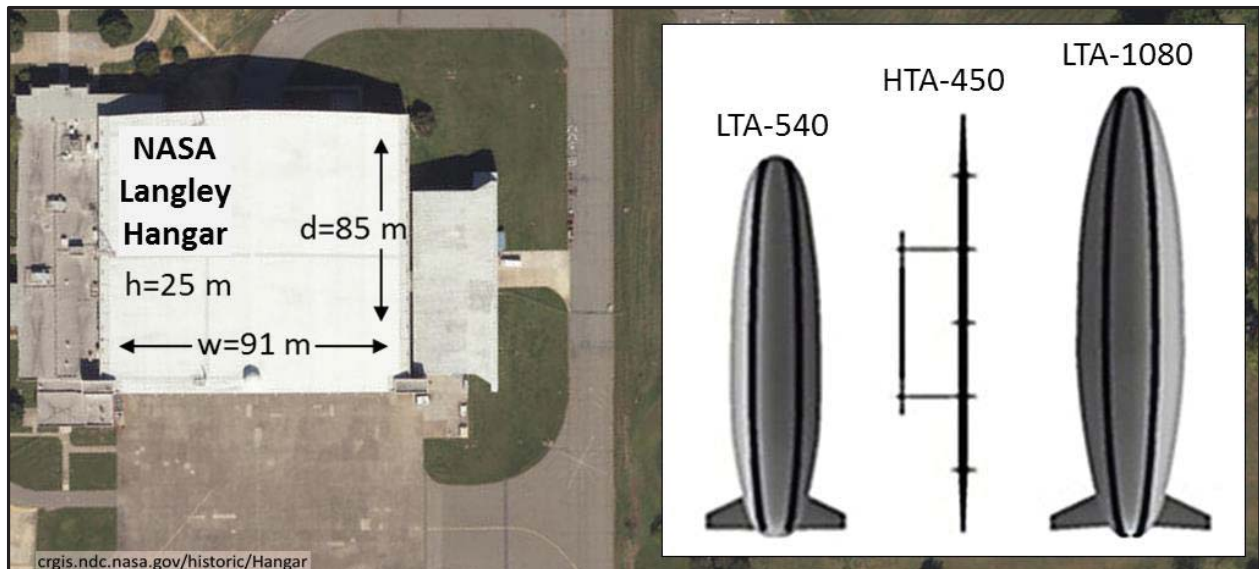
Figure 34. Scaled top-views of three HALE UAV concepts compared to NASA Langley Hangar.

Figure 35. Scaled side-view of LTA-1080 outside NASA Langley Hangar.

5.0 Mission Simulation Results and Discussion

This section describes the various station-keeping missions defined for this study, carried out using the HTA-450, LTA-1080, and LTA-570 vehicle concepts discussed in the previous section. The capability of each vehicle to complete the simulated mission objectives was determined based on a number of operational performance metrics, such as the energy availability and station-keeping persistence. The results are configured to facilitate comparisons of the specific capabilities and limitations of each vehicle concept. Results can be alternately interpreted to bound the operational suitability of a particular vehicle concept, or to identify which vehicle concept is most suitable for completing a particular mission.

5.1 Mission Descriptions

Figure 36 is a map of the seven geographically distributed mission sites selected for this study. The sites were selected to provide variations in latitude and longitude from a group of candidate NCDC sites with plentiful long-term atmospheric measurements. At high altitudes, mission atmospheric conditions vary as a function of season, altitude, latitude, and longitude whereas mission solar flux varies primarily as a function of season and latitude. In the northern hemisphere, high altitude winds are strongest above the northeastern regions of Asia and North America. Seasonally, the strongest winds occur during the winter months, concurrent with the shortest length of day and lowest Sun angles, whereas the weakest winds occur during the summer months. Table 6 lists the site name, latitude, longitude and the approximate duration of the shortest day at the site latitude, and mission simulation details.

Table 6. Site and Mission Details

Site Name	Latitude N (deg.)	Longitude W (deg.)	Shortest Day (approximate)	Day1 - Day30 (2009) 30-Day Missions	Jan. 1 - Dec. 31 (2009) 1-Year Mission	(NCDC Data) Wind Year
Spokane, WA	47.7	117.7	8h 20m	√	no	2009
Green Bay, WI	44.5	88.1	8h 45m	√	√	2009
Reno, NV	39.6	119.8	9h 20m	√	no	2009
Topeka, KS	39.1	95.6	9h 25m	√	no	2009
Wallops Island, VA	37.9	75.5	9h 30m	√	√	2009
Santa Teresa, NM	31.9	106.7	10h 5m	√	√	2009
Jacksonville, FL	30.5	81.7	10h 10m	√	no	2009

Figure 36. Mission sites map.

High altitude missions with durations of 30 days were simulated at each site for all vehicle concepts. Due to variations of the atmospheric and solar environment throughout the year, four separate, seasonal 30-day missions were simulated at each site during the summer, fall, winter, and spring. Also, 1-year missions

starting on January 1, 2009 and ending on December 31, 2009 were simulated at Green Bay, Santa Teresa and Wallops Island for all vehicle concepts.

5.2 Mission Simulation Results and Discussion

The mission time-integrated WindData%, AvEnrg%, and PwrRad% metrics are listed for each simulated mission in Table 7, Table 8, and Table 9, respectively. For enhanced visualization, percentage values < 70% are shaded pink to indicate poor performance, values ≥ 90% are shaded green to indicate good performance, and intermediate values are shaded yellow. Below each table, the WindData%, AvEnrg%, and PwrRad% metrics are also plotted per mission site as bar graphs in Figure 37, Figure 38, and Figure 39, respectively. These parameters are mission-time integrated outputs and are used as the primary metrics for assessing overall mission performance.

The WindData% suitability metric is defined as the fraction of mission time steps utilizing NCDC historical data divided by the total number of mission time steps. The metric was developed to provide the feedback necessary to assess the extent to which either measured conditions or approximated median atmospheric conditions are incorporated to a given mission simulation. The WindData% suitability metric and the number of timesteps utilizing approximated median conditions are both listed in the SolFlyte output file. Relatively low WindData% values can indicate the need for in-depth review of the input mission wind data quality. The WindData% suitability metric also can vary for dissimilar vehicles operating at identical mission sites and times. This can occur because the vehicle performance dictates access to different operational altitudes, including those differences associated with the simulated mission wind data availability at those altitudes. In such cases, WindData% output values can indicate the need to review the interactions between mission operational constraints and vehicle performance capabilities. Table 7 indicates that quality historical wind data was accessible for most vehicle concepts and missions of this study. For the HTA-450 vehicle concept, WindData% values ranged from 94% to 100% for the 30-day missions and from 98% to 100% for the one-year missions. With the exception of four 30-day missions, WindData% values associated with all missions executed using the LTA-1080 vehicle concept range from 91% to 100%. The wind data quality for the 30-day Spokane mission in December was acceptable, but the data were sparse, thus causing the lowest WindData% value of 66%. The WindData% values are relatively low for six of the 30-day LTA-570 missions during December and March, but range from 92% to 100% for all other missions. The wind data quality for the 30-day Spokane mission in December was similar to the LTA-1080 vehicle. Other moderately low WindData% values are caused by data gaps at the low operating altitudes of the LTA-570 that are not present at higher altitudes accessible to the LTA-1080 or HTA-450.

The mission time-integrated AvEnrg% availability metric, discussed earlier, is the fraction of time steps that energy had been available to power all required mission operations, divided by the total number of mission time steps. Note that the power could be generated from either ESS reserves, direct solar-electric, or a combination of reserves and direct solar energy. For all time steps when the energy availability status parameter value (also described previously, in Table 1) was not greater than zero, the vehicle would have required additional energy availability, whether or not the vehicle had been on station. From a design standpoint, the vehicle design would require modifications to store or collect energy in order to generate power for the duration of the mission, provided other design factors were constant.

Table 7. Mission Time-Integrated NCDC Wind Data Suitability Metric, WindData%

| WindData%		December			March			June			September			Jan 1 - Dec 31		
Latitude	Site	H 450	L 1080	L 570	H 450	L 1080	L 570	H 450	L 1080	L 570	H 450	L 1080	L 570	H 450	L 1080	L 570
N 48°	Spokane	94	66	71	97	80	79	100	100	100	99	100	100			
N 45°	Green Bay	94	100	88	98	82	82	100	100	100	100	100	100	98	100	96
N 40°	Reno	96	76	86	99	91	92	100	97	97	100	100	100			
N 39°	Topeka	96	96	83	94	93	93	99	100	100	96	96	96			
N 38°	Wallops	98	100	98	99	97	97	100	98	98	100	100	100	98	100	97
N 32°	Santa Teresa	100	100	100	100	100	100	100	100	100	100	98	98	100	100	100
N 30°	Jacksonville	98	97	97	99	100	100	100	100	100	97	99	99			
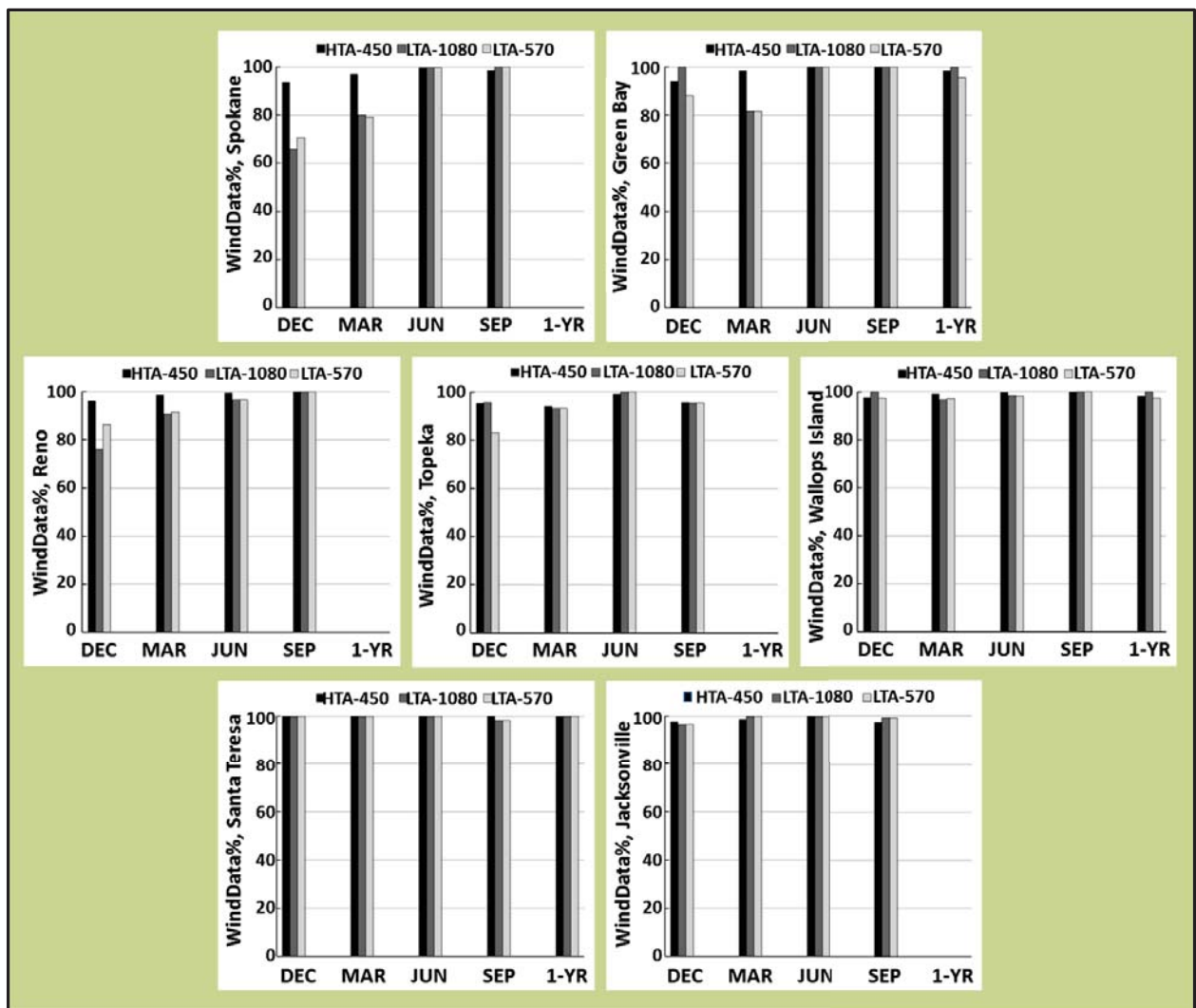
Figure 37. NCDC wind data suitability metric per mission site.

Table 8. Mission Time-Integrated Energy Availability Metric, AvEnrg%

| AvEnrg%		December			March			June			September			Jan 1 - Dec 31		
Latitude	Site	H 450	L 1080	L 570	H 450	L 1080	L 570	H 450	L 1080	L 570	H 450	L 1080	L 570	H 450	L 1080	L 570
N 48°	Spokane	30	56	38	73	97	81	100	99	99	82	100	100			
N 45°	Green Bay	37	45	33	76	86	69	100	100	100	85	100	100	74	82	76
N 40°	Reno	46	64	56	81	99	97	100	100	100	89	100	100			
N 39°	Topeka	47	51	43	81	90	80	100	100	100	89	100	100			
N 38°	Wallops	47	50	32	82	94	75	100	100	100	90	100	100	79	85	80
N 32°	Santa Teresa	58	75	64	86	96	87	100	100	100	93	100	100	83	96	91
N 30°	Jacksonville	60	85	70	88	100	99	100	100	100	94	100	100			
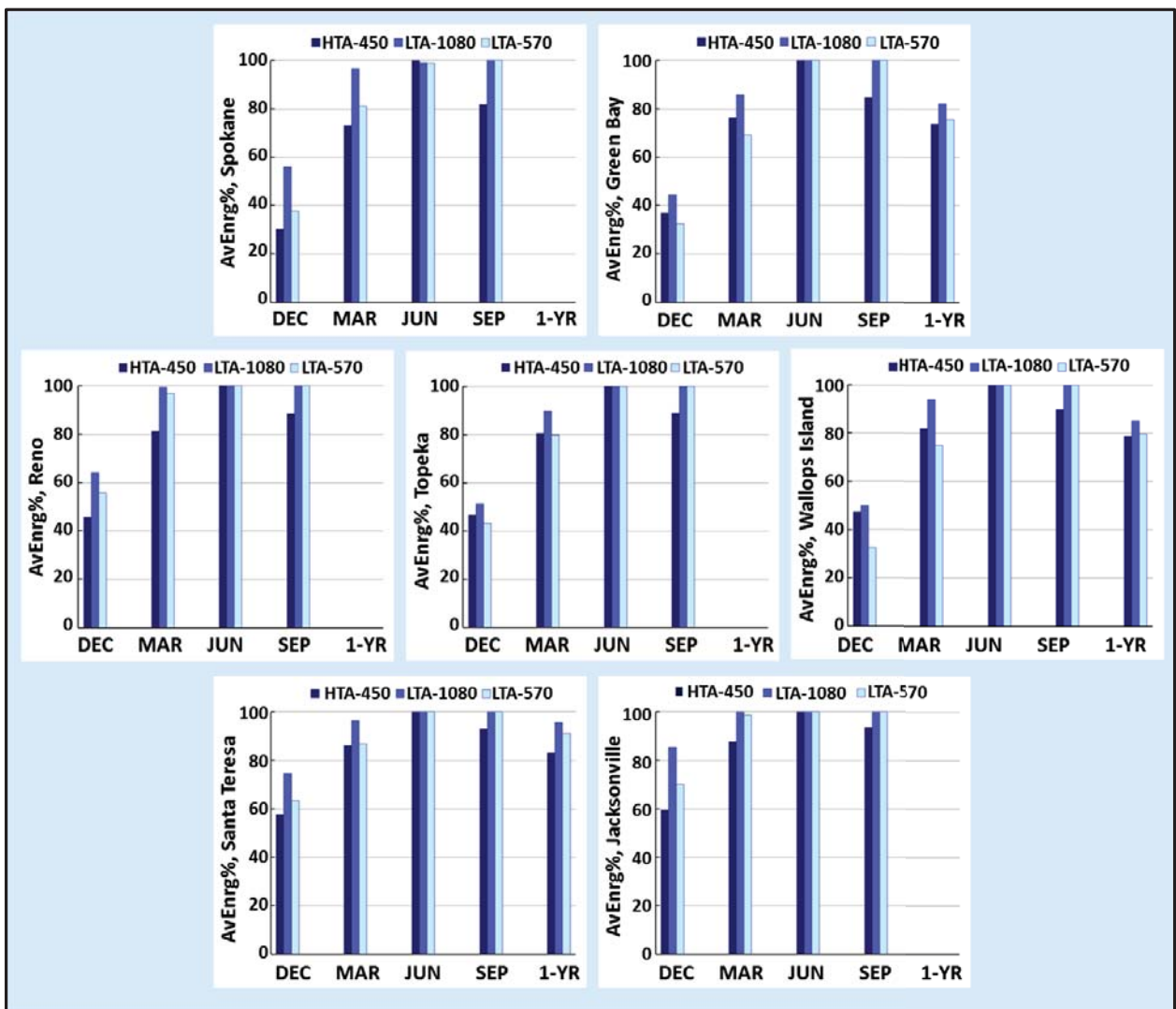
Figure 38. Energy availability metric per mission site.

44

Table 9. Mission Time-Integrated Power-Radius Capability Metric, PwrRad%

| PwrRad%		December			March			June			September			Jan 1 - Dec 31		
Latitude	Site	H 450	L 1080	L 570	H 450	L 1080	L 570	H 450	L 1080	L 570	H 450	L 1080	L 570	H 450	L 1080	L 570
N 48°	Spokane	100	100	26	100	100	85	100	100	100	100	100	100			
N 45°	Green Bay	64	56	51	100	96	65	100	100	100	100	100	100	87	84	74
N 40°	Reno	96	67	35	99	100	100	100	100	100	100	100	100			
N 39°	Topeka	61	55	50	99	86	47	100	100	100	100	100	100			
N 38°	Wallops	42	24	22	100	86	64	100	100	100	100	100	100	87	78	71
N 32°	Santa Teresa	71	67	23	100	100	80	100	100	100	100	100	100	95	95	86
N 30°	Jacksonville	74	100	43	100	100	100	100	100	100	100	100	100			
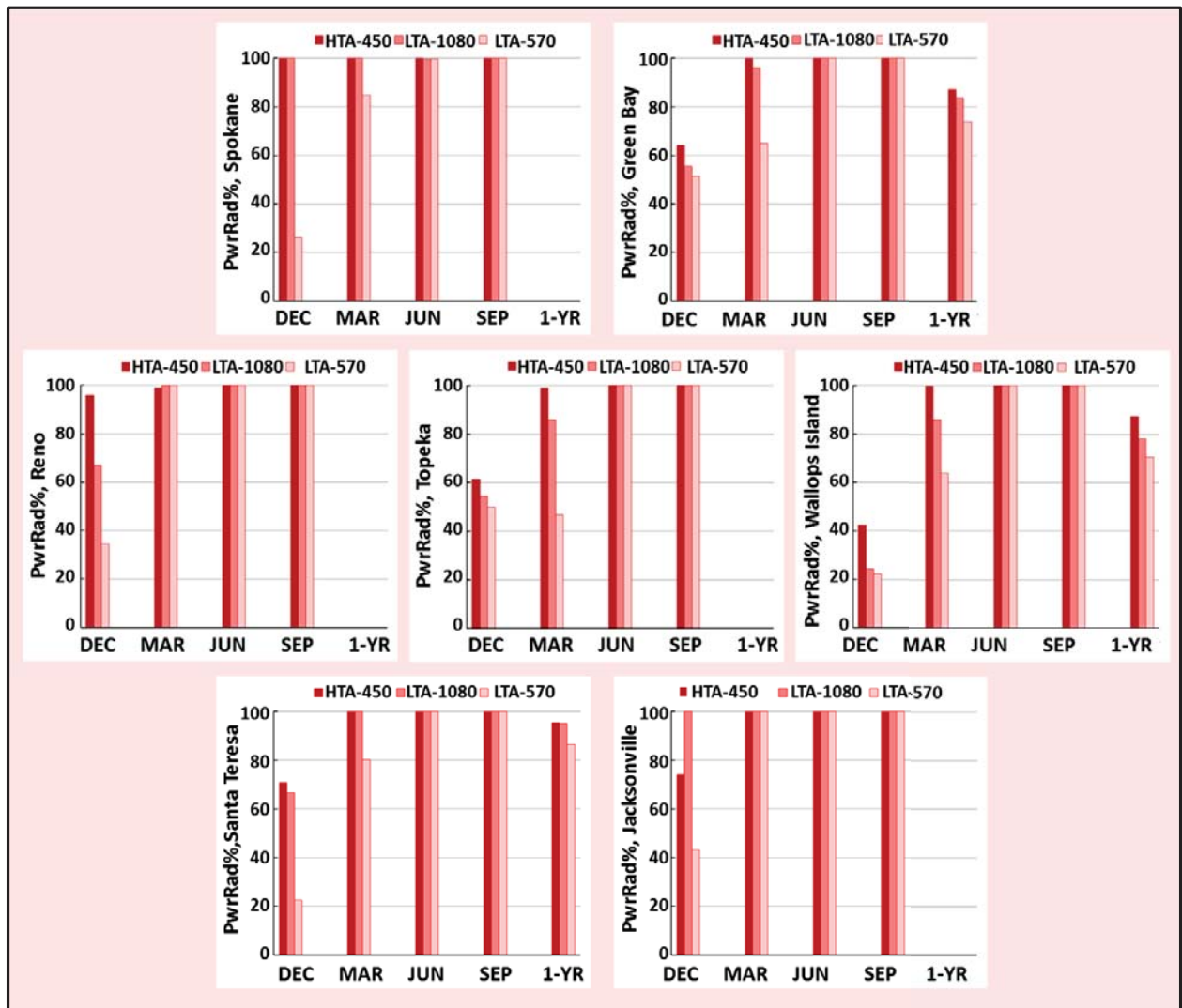
Figure 39. Power-radius capability metric per mission site.

The PwrRad% capability metric indicates the percentage of the mission time the vehicle is within the specified radial distance of 36 km from the mission site and provides a measure of the capability of the vehicle to operate in the mission winds occurring during the simulated mission. Results indicate that the

45

HTA-450 AvEnrg% is only 30% during the December mission at Spokane; however, if the AvEnrg% metric had been equal to 100%, the HTA-450 would posess the capability for station-keeping during 100% of that mission. In contrast, the available solar energy collection and limited performance capabilities of the LTA-570 would provide a PwrRad% capability of 26% and an AvEnrg% availability of only 38% during a mission in December at Spokane. As a result, the combined effects would enable station-keeping during this mission for a maximum of 26% of the time. As the two metrics do not necessarily overlap as a function of mission time, the operational station-keeping would likely be less than 26%. This examplifies how station-keeping qualities can be separately considered, and points to the need to properly size the ESS capacity and solar arrays as the first step toward station-keeping functionality.

Examination reveals a few clear trends; all of the vehicles struggle to close the energy cycle and maintain energy availability during the month of December, regardless of location. As winter solstice occurs on December 21, these days provide the least amount of daylight and solar energy relative to any other time of the year at these locations. Adding energy storage capacity leads to a short term delay toward energy depletion, as the underlying issue is the ability to collect sufficient solar energy during December. On the contrary, all of the vehicles successfully completed the mission during the month of June, which encompasses the summer solstice and has the longest days of the year at these locations. March provides the most interesting results as the environmental conditions are challenging, but not overwhelming. Although the astronomical conditions are similar, spring wind speeds delineate March mission results from the almost summer-like September mission results. It is possible to note some latitudinal trends during March as overall performance of all the concepts improves from northern sites to southern sites. The LTA-1080 demonstrates the best AvEnrg% performance, and is appropriately sized for mid- to low-latitude missions during the period March through September. The LTA-570 AvEnrg% availability drops slightly compared to the LTA-1080, and is more comparable to the HTA-450. In terms of on-station performance however (Figure 39), the HTA-450 consistently out-performs the LTA concepts because of the faster operational speeds, with the exception of the LTA-1080 mission at Jacksonville in December. This particular exception was investigated in more detail, as discussed below.

Consider the PwrRad% capability associated with the HTA-450 and LTA-1080 missions during December at Jacksonville, shown in Table 9, as 74% and 100%, respectively. The result might seem counter-intuitive within the context of the operational capabilities of LTA and HTA concepts. As discussed previously, HTA vehicles are especially well-suited to climbing and descending in order to seek more advantageous atmospheric conditions, or to store potential energy during the daytime. Conversely, LTA vehicles are limited to a narrow band of operating altitudes just above and below the level of neutral buoyancy. However, operational rules can dictate when the simulation will access a particular altitude, assuming sufficient vehicle performance capabilities and energy reserves.

During this mission, the wind speeds were quite strong at the 100 mb level, and were moderate at the 70 mb and 50 mb levels. Although the HTA concept was capable of accessing all three flight levels, the maximum altitudes were limited to provide similarity to the LTA operational capability to access only the 100 mb and 70 mb flight levels. As a result, the LTA concept operated at the 70 mb pressure altitude during all times of fast wind speeds at 100 mb. On the other hand, by enforcing an HTA altitude ceiling to provide fair comparisons, the HTA vehicle concept was not always able to access the higher altitudes for operations during fast wind speeds at a pressure altitude of 100 mb, although performance capabilities would have enabled such operations. The situation was such that the LTA concept could remain on-site for the entire mission. However, the HTA vehicle was capable of climbing to higher altitudes during the morning only if the net energy balance had been greater than 0 kWh. Thus, the altitude profile of the HTA-450 during periods of high winds followed the repeating pattern of: daytime climbing to 50 mb, early evening descending to 70 mb, nighttime continued descent to100 mb, and then early morning climbing to 70 mb. As a result of these two factors, the HTA vehicle remained on-site during some, but not all, of the time that the wind speeds were excessively fast at the 100 mb level.

The HTA-450 would exhibit 100% on-site capability at all mission sites and all times of year, except during December when the wind speeds increase. The LTA-1080 and LTA-570 struggle during the stronger winds that occur during winter and spring. In some cases, the LTA-570 is on-site for less than 30% of the total mission time. Finally, none of the concepts were capable of station-keeping for 100% of the time during the one-year duration mission simulations. The HTA-450 showed the best overall performance during the one-year missions, followed by the LTA-1080 and LTA-570.

Mission Orientations for the HTA-450 and LTA-1080 Concepts

The relative orientations from the HTA-450 and the LTA-1080 vehicle concepts to the Sun are shown in Figure 40 for each of the 30-day seasonal missions simulated at Wallops Island, VA. Figure 41 shows the same information for the 30-day seasonal missions simulated at Santa Teresa, NM. Both figures include all outbound and return orientations for every mission time step when the solar altitude angle was calculated to be greater than approximately -10º (about 5º below the horizon at the mission altitudes). Seasonal variability is evident in the shapes of the energy-optimal orientations for both the HTA and LTA concepts at both mission sites shown here. Also, the shapes of the HTA and LTA relative orientations to the Sun are notably different.

In all cases, the HTA orientations trend toward the preferred orientations of 90º and 270º. The faster wind speeds that were encountered during the winter (December) and spring (March) cause the vertical band of mission orientations to widen in accordance with the discussions regarding Figure 14. As would be expected, the vertical band stretches and contracts depending on the maximum solar altitude angle during the particular season. At low solar altitude angles, the width of the energy optimal orientations expands to avoid regions of localized energy collection minima. Also, because the absolute energy collection is low, the HTA-450 vehicle concept loses the option to expend energy overcoming even light winds, in order to access more energy efficient orientations.

It is possible that some scatter might result from coarsely modeling the speed increment as 2 m/s and the heading increment as 10º. It was hypothesized that a finer speed increment of perhaps 0.5 m/s and a finer heading increment of 3º might more precisely constrain the orientations. Several new tests cases were evaluated at the completion of this study to test the hypothesis. Initial analysis of the results indicated that using a vehicle speed increment of 0.5 m/s changed the optimal mission flight orientations, but not significantly. However, changing the heading increment to 3º resulted in noticeably more constrained patterns. This will be a consideration at the outset of future studies when the mission simulation parameters are defined.

The LTA relative orientations are shaped by the vehicle and array geometry that leads to generally horizontal contours with less pronounced preferred orientations. Perhaps more importantly however, the SolFlyte-LTA model provides the capability to access solar orientations that are offset from the flight path. In other words, the LTA vehicle concept can rotate around the z-axis as it slowly drifts or floats above the mission site. Finally, during periods of high winds, the LTA concept is rapidly constrained to recoverable flight patterns that are directly aligned with the wind vector heading. This is most evident in the results of the 30-day December mission at Wallops Island, VA.
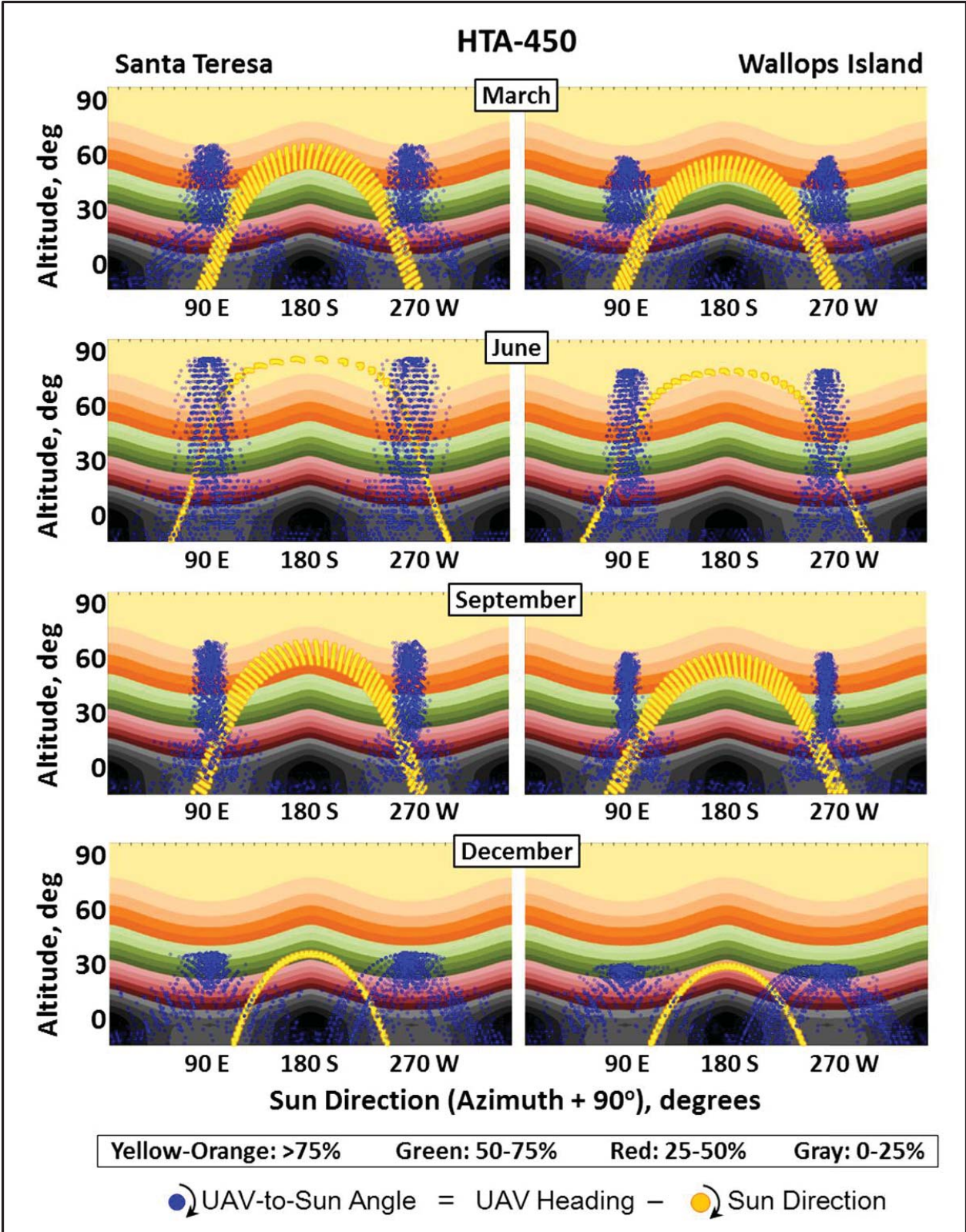
Figure 40. HTA-450 orientations to the Sun, 30-day Santa Teresa and Wallops Island missions.
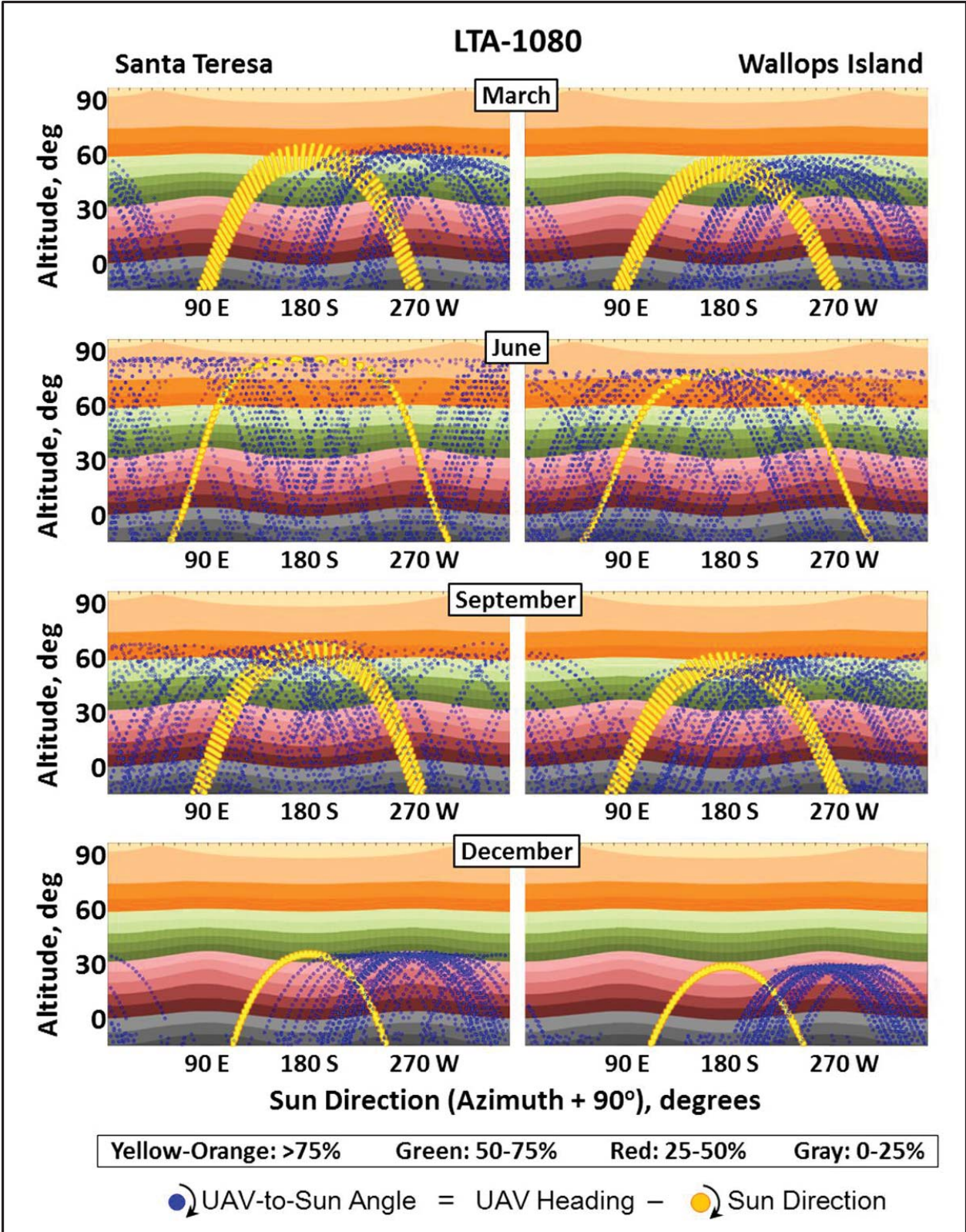
Figure 41. LTA-1080 orientations to the Sun, 30-day Santa Teresa and Wallops Island missions.

Wind Speed Variations Throughout the Years

The atmospheric conditions of this study were based on high-altitude measurements obtained at selected NCDC stations featuring long-term observation programs and a particularly full complement of data from the calendar year 2009. If the station-keeping results of this study are to be deemed as applicable benchmarks for similar missions in other years, then the 2009 conditions must be proven as representative of the conditions in other years. As daily, seasonal, and annual unpredictability is a certainty of weather, using only 2009 atmospheric data suggests the need to enhance the analysis procedure when determining station-keeping capabilities during other years.

Previous research within the ASAB indicates that wind speed can be modeled as a probablisitic Rayleigh distribution, but this neglects the importance of time dependence. Neglecting time removes the ability to determine how many hours light, average, or maximum winds will persist, or if the wind speeds and durations (at those speeds) are correlated. For an existing vehicle operating at the mission site, it might be possible to forecast how long winds will blow and at what speeds. However, when designing a new vehicle, this phenomenon must be modeled and somehow implemented during the concept development phase. Without such considerations, a stated design requirement for station-keeping persistence during maximum wind speeds for maximum durations could risk burdening the design concept with constraints that might lead to over-design and excessive cost, or worse, a seemingly unachievable design objective.

To generalize and extend the applicability of the PwrRad%, AvEnrg%, and any other similarly defined metric, missions should be simulated for multiple years at the same mission site, during the same mission period to obtain a range of values for each metric. The average value of each metric provides the final indication of station-keeping performance, including the effects of annual weather variations.

6.0 Conclusions

A new and unique complex modeling capability has been developed that is suitable for the analysis of solar powered high altitude long endurance concepts, including both HTA and LTA configurations. The SolFlyte analysis tool includes the effects of winds aloft, solar position and flux, recoverable flight patterns, vehicle-to-Sun orientations, and vehicle self-shadowing, all as a function of time and mission location. This capability was utilized to investigate the design and performance trades required when comparing HTA and LTA concepts. Results indicate that:

- The HTA concept attained longer periods of on-site persistence than either LTA concept, as indicated by the power-radius capability metric, PwrRad%.

- The LTA concepts provided more reliable energy availability than the HTA concept, as indicated by the energy availability metric, AvEnrg%, but these energy benefits required prohibitive design trades of reduced performance (LTA-570) or excessive solar array area (LTA-1080).

A summary of the design trade-off information is shown in Table 10. The LTA concepts are larger and heavier, and achieving the same performance requires substantially more solar array area (LTA-570 vs. LTA-1080). The LTA-1080 is of similar mass as the HTA-450 concept, yet the array area exceeds the array area of the HTA-450 concept. This would introduce a substantial cost component to the LTA vehicle concept selection. Although the wingspan of the HTA concept is roughly equivalent to the length of the LTA concepts, the volumes of the LTA concepts dictate the need for a larger hangar volume. New facility

construction costs or the availability of a larger hangar must be included when considering the selection of LTA concepts. As a result, it is likely that the LTA-1080 concept would be more costly to build and operate than the HTA concept. In contrast, during operational periods of light winds, LTA concepts can float in place with little power required to maintain position or altitude, thus reducing the burden of energy availability and storage. The advantages of utilizing an HTA or LTA vehicle concept are clearly indicated by the energy availability metric, AvEnrg%, and the power-radius capability metric, PwrRad%, results for the one-year duration missions summarized below.

Table 10. Vehicle and Mission Summary

Parameter	HTA-450	LTA-1080	LTA-570	Units
Wingspan	127	-	-	m
Length	25	135	115	m
Width	-	32	27.5	m
Height	7.5	37	32	m
Takeoff Gross Mass	3854	6854	4317	kg
Solar Array Area	450	1080	570	m2
Maximum Speed	40.6	36.0	32.0	m/s
Minimum Speed	31.7	0.1	0.1	m/s
Green Bay, 1-Year Mission				
AvEnrg%	73.7	82.0	75.6	%
PwrRad%	87.1	83.7	73.9	%
Santa Teresa, 1-Year Mission				
AvEnrg%	83.1	95.6	91.2	%
PwrRad%	95.3	95.0	86.4	%
Wallops, 1-Year Mission				
AvEnrg%	78.9	85.1	79.6	%
PwrRad%	87.4	78.1	70.5	%

Selecting a preferred HTA or LTA vehicle concept depends on the mission objectives and constraints, particularly the desired levels of station-keeping persistence, the mission time of year, and the mission operational site. Large LTA concepts can host the required ESS capacity and solar array area with less impact to the design, and can provide the capability to float over targets for long periods of time; however, station-keeping becomes difficult when winds aloft increase. The HTA concept operates at faster speeds, greater than the stall speed of about 32 m/s, and inherently provides better station-keeping persistence, as indicated by higher values of the power-radius capability metric, PwrRad%. Both HTA and LTA vehicle concepts could prove useful as cost effective platforms for future HALE UAV missions.

References

1. Nickol, C.; Guynn, M.; Kohout, L.; and Ozoroski, T.: High Altitude Long Endurance Analysis of Alternatives and Technology Requirements Development. NASA/TP-2007-214861, March 2007.

2. Ozoroski, T.; and Mas, K.: A PC-Based Design and Analysis System for Lighter-Than-Air Unmanned Vehicles. AIAA-2003-6566, September 2003.

REPORT DOCUMENTATION PAGE

Form Approved
OMB No. 0704-0188

1. REPORT DATE *(DD-MM-YYYY)*	2. REPORT TYPE	3. DATES COVERED *(From - To)*
01-01-2015	Technical Memorandum	

4. TITLE AND SUBTITLE

High Altitude Long Endurance UAV Analysis Model Development and Application Study Comparing Solar Powered Airplane and Airship Station-Keeping Capabilities

5a. CONTRACT NUMBER

5b. GRANT NUMBER

5c. PROGRAM ELEMENT NUMBER

6. AUTHOR(S)

Ozoroski, Thomas A.; Nickol, Craig L.; Guynn, Mark D.

5d. PROJECT NUMBER

5e. TASK NUMBER

5f. WORK UNIT NUMBER

526310.04.07.04

7. PERFORMING ORGANIZATION NAME(S) AND ADDRESS(ES)

NASA Langley Research Center
Hampton, VA 23681-2199

8. PERFORMING ORGANIZATION REPORT NUMBER

L-20515

9. SPONSORING/MONITORING AGENCY NAME(S) AND ADDRESS(ES)

National Aeronautics and Space Administration
Washington, DC 20546-0001

10. SPONSOR/MONITOR'S ACRONYM(S)

NASA

11. SPONSOR/MONITOR'S REPORT NUMBER(S)

NASA-TM-2015-218677

12. DISTRIBUTION/AVAILABILITY STATEMENT

Unclassified - Unlimited
Subject Category 05
Availability: NASA STI Program (757) 864-9658

13. SUPPLEMENTARY NOTES

14. ABSTRACT

There have been ongoing efforts in the Aeronautics Systems Analysis Branch at NASA Langley Research Center to develop a suite of integrated physics-based computational utilities suitable for modeling and analyzing extended-duration missions carried out using solar powered aircraft. From these efforts, SolFlyte has emerged as a state-of-the-art vehicle analysis and mission simulation tool capable of modeling both heavier-than-air (HTA) and lighter-than-air (LTA) vehicle concepts. This study compares solar powered airplane and airship station-keeping capability during a variety of high altitude missions, using SolFlyte as the primary analysis component. Three Unmanned Aerial Vehicle (UAV) concepts were designed for this study: an airplane (Operating Empty Weight (OEW) = 3285 kg, span = 127 m, array area = 450 m2), a small airship (OEW = 3790 kg, length = 115 m, array area = 570 m2), and a large airship (OEW = 6250 kg, length = 135 m, array area = 1080 m2). All the vehicles were sized for payload weight and power requirements of 454 kg and 5 kW, respectively. Seven mission sites distributed throughout the United States were selected to provide a basis for assessing the vehicle energy budgets and site-persistent operational availability. Seasonal, 30-day duration missions were simulated at each of the sites during March, June, September, and December; one-year duration missions were simulated at three of the sites. Atmospheric conditions during the simulated missions were correlated to National Climatic Data Center (NCDC) historical data measurements at each mission site, at four flight levels.

15. SUBJECT TERMS

Airship; Climatology; High altitude; Solar powered aircraft; System analysis

16. SECURITY CLASSIFICATION OF:			17. LIMITATION OF ABSTRACT	18. NUMBER OF PAGES	19a. NAME OF RESPONSIBLE PERSON
a. REPORT	b. ABSTRACT	c. THIS PAGE			STI Help Desk (email: help@sti.nasa.gov)
U	U	U	UU	61	19b. TELEPHONE NUMBER *(Include area code)* (443) 757-5802

Standard Form 298 (Rev. 8-98)
Prescribed by ANSI Std. Z39.18